AD 295 889

THE PENNSYLVANIA STATE UNIVERSITY
Department of Engineering Mechanics

PROGRESSING WAVE ANALYSIS OF BLAST WAVES IN SPHERES

TECHNICAL REPORT NO. 1

DEPT. of the ARMY PROJECT No: DA-36-034-ORD-3576RD

ORD. MANAGEMENT STRUCTURE CODE NO: 5010.11.81500.01

by

NORMAN DAVIDS and HARRY H. CALVIT

November 30, 1962

Technical Supervision by

Aberdeen Proving Ground, Maryland

Ballistic Research Laboratories

UNCLASSIFIED

UNCLASSIFIED

TECHNICAL REPORT NO. 1

November 30, 1962

PROGRESSING WAVE ANALYSIS

of

BLAST WAVES IN SPHERES

November 30, 1962
(Unclassified)

by

Norman Davids and Harry H. Calvit

DEPT. of the ARMY PROJECT No: DA-36-034-ORD-3576RD
ORD. MANAGEMENT STRUCTURE CODE NO: 5010 11 81500.01

THE PENNSYLVANIA STATE UNIVERSITY
Department of Engineering Mechanics

Technical Supervision by

Ballistic Research Laboratories
Aberdeen Proving Ground, Maryland

UNCLASSIFIED

BALLISTIC RESEARCH LABORATORIES

THE PENNSYLVANIA STATE UNIVERSITY

PROJECT NO: DA-36-034-ORD-3576-RD

Progressing Wave Analysis of Blast Waves in Spheres

Report No. 1

ABSTRACT

A theory of crater formation by impact awaits better understanding of the process of shock-wave propagation in solids, especially waves with spherical symmetry. This paper studies theoretically and experimentally the non-steady motion of metallic spheres initiated by explosive blast in a spherical cavity. The method of progressing waves is applied to determine the radius versus time diagram of the propagation of the wave into the material and leads to values for cavity sizes. The assumptions are made that the material in the vicinity of the cavity possesses a polytropic equation of state, that entropy is constant for an element of material, and that the total energy is constant in time. The original partial differential equations of the problem are then reducible to a succession of ordinary differential equations. Using the Rankine-Hugoniot relations as initial conditions at the shock front, these equations have been integrated using a numerical program developed for a number of metals and the construction of r,t-diagrams carried out with values for particle velocities and pressure variation on the inner surface. The solutions of the differential equation of progressing waves have been studied by constructing a solution diagram, which is similar to a hodograph plane. An analysis was made of this plane and the role played by the singularities of the differential equation. The appropriate solution curve starts very close

to a positive node of the equation, then approaches very close to a saddle-type singularity in a corner of the plane which has been found to represent a meaningful physical boundary condition, namely that pressure and velocity tend asymptotically to zero with increasing time in the proper manner.

Using an equation of state for aluminum (obtained from data from Los Alamos publications) there is obtained the expansion of a cavity of 1.7 cm radius in a thick aluminum sphere, filled with 31.6 grams of Pentolite, to its final measured value of 3.0 cm. The initial pressure, which is of the order of 300 kilobars, drops to less than 100 kb in less than 2 microseconds. At this time the shock velocity drops to its acoustic or elastic value in the material. However, the cavity continues to expand to its final stage in a time of 80 microsec. The simultaneous drop of pressure, velocity, and departure of the medium from the polytropic equation of state signals the termination of the shock regime This appears as a triangular region on the r,t-diagram, bounded by the shock front, the inner cavity, and the line t = 2 microsec. Beyond this time the material of the zone continues to flow radially outwards essentially as an incompressible fluid.

The assumption that metals behave similar to gases as a result of an explosion or impact, is limited to this shock zone, which is shorter in duration than may have been expected From the known outward displacements of the outer radius of the sphere ≈ .1 inch) the increase in cavity volume is accounted for geometrically.

A similar time scale of events may be expected to take place in an impact crater, that is, the shock wave regime should be terminated essentially before the flow of material both radial and tangential, has started.

The Ballistic Research Laboratory, Aberdeen Proving Grounds, is conducting a parallel experimental program on thick aluminum spheres and have furnished data needed for this analysis.

TABLE OF CONTENTS

LIST OF SYMBOLS

p, P	pressure
ρ	density
ρ_o	initial density
t	time
r	radius
u	radial "particle" velocity
c	sound velocity
V	volume
V_o	initial volume
γ	adiabatic exponent
A	constant in polytropic gas relation
α, β, δ, ϵ	progressing wave exponents
$\xi = rt^{-\alpha}$	progressing wave parameter
U, D, P	progressing wave functions
Δ	$= (U - \alpha)^2 - \gamma P$
N, Q, R, S	functions of U, see (4.8b)
μ	$= \sqrt{(\gamma - 1)/(\gamma + 1)}$
E	energy
kb	kilobars
s	arc length
C	shock wave velocity

1. INTRODUCTION - Description of the Problem

The Ballistic Research Laboratory (BRL), Aberdeen Proving Grounds, is engaged in conducting an experimental program of internal explosions in small cavities in metal spheres. The aim of this report is to give the results of an analytical study of the problem, with particular emphasis on the propagation of shock waves in the metal immediately after detonation of the explosive.

Figs. 1 and 2 show a 7 inch sphere of aluminum such as has been used to date in BRL experiments. The phenomena, and hence their analysis, which result from detonation of the explosive in the inner cavity, are complex because different effects predominate in different parts of the material. Thus, there is an innermost zone or spherical shell where very large radial displacements have occurred under temperatures and pressures far beyond the range of conventional mechanical behavior. The material is in some type of "fluid" state in this zone and shows relatively little tendency for cracks to initiate there. Next, there is an intermediate zone of the sphere where displacements have dropped to elastic ranges and where brittleness seems to have returned, as evidenced by the many small tension and shear cracks which have formed there. A few of the stronger cracks which get started may penetrate into the adjacent regions and ultimately reach the boundaries. Finally, there is an outermost zone dominated by the effect of the external boundary of the sphere. Here reflection effects such as scabbing cracks are often observed.

The transition between successive zones are not exact, but in some specimens, rather surprisingly enough, are fairly sharply delineated.

In this report we shall make an analysis of the innermost shock zone. Its direct aim is to provide a description of the shock process in the

metal. More specifically a useful theory must furnish a time for the duration of the process, the size of the zone influenced by the shock front, values for the displacements, and thermodynamic variables of pressure, density, and temperature in the material. A useful tool is the r,t-diagram which shows the path made by a set of concentric spherical shells. This diagram is possible because of the single space coordinate.

The problem of the shock expansion of spherical cavities is closely related to that of crater formation by hypervelocity projectiles. The features we have outlined above are present in the crater problem as well. The crater problem carries with it, however, the further complication of tangential flow, thus requiring two space coordinates. Except for the presence of the plug shown in Figs. 1 and 2, the arrangement for the blasts have spherical symmetry, and we may confidently assert that radial motion occurs, so that all the physical quantities of the problem depend on only one space coordinate. There is however, a slight actual departure because of the plug or because of asymmetrical detonation, and which are not important to the problem.

2. Spherical Shocks - Time Sequence of Effects

Just as the study of the problem has been conveniently divided up into spatial zones, we can divide up the sequence of events in the spherical blast process for detailed analysis as follows:

a) Initial Stage - Here the detonation wave of the exploding gas starts contact with the solid and then generates a shock wave in the solid. This stage might be considered as terminated when the density in the solid has dropped to its free space value, at the inner cavity.

b) Expansion Stage - The compressed solid expands radially outward and actually forms the cavity. This stage is dominated mostly by inertia forces.

c) Final Stage - Here the shock wave decays, permanent deformation of the cavity stops, and the material has undergone some permanent plastic strain.

The first stage lasts up to about 2.5 micro-seconds. The second turns out to be relatively long and can take up to about 100 microseconds or even longer. It must, of course, be understood that these phases need not be distinctly separated events in time, especially the terminating phase of the expansion.

3. Basic Mathematical Equations of Shock Waves

Because of spherical symmetry our problem is reducible to a radial and a time coordinate. Shock wave propagation in a solid is very closely related to that of a spherical wave in a gas. We may make the following assumptions about the medium:

1. Thermodynamic equilibrium holds (See [2], p. 3), i.e. that changes of state are adiabatic By this we mean that entropy is constant along a "particle path", i.e., a fixed element of the medium.

2. The medium is a perfect fluid, i e., any rigidity or shear effects are neglected.

3. The effects of entropy changes are negligible, i.e., that the pressure is a function of the density alone (the medium is said to be barotropic).

4. The total energy available for the motion is fixed.

The conservation laws for an element of material expressed in Lagrangean form, i.e., along the particle paths, are as follows:

$$d\rho/dt = -\rho(\partial u/\partial r) - 2u\rho/r = -(\rho/r^2)\partial(r^2u)/\partial r \qquad (3.1)$$

(mass)

$$du/dt = -\partial p/\rho\partial r \qquad \text{(momentum)} \qquad (3.2)$$

$$f(P,\rho) = 0 \quad \text{or} \quad df/dt = 0 \qquad \text{(eq. of state)} \qquad (3.3)$$

Thus if the medium were assumed to be polytropic with the adiabatic exponent γ, we would have, for (3.3),

$$f(p,\rho) = p\rho^{-\gamma} = \text{const.} = A \qquad (3.4)$$

These equations, in Eulerian form, with subscripts denoting partial derivatives, become

$$\rho_t + u\,\rho_r + \rho u_r + 2u\rho/r = 0 \qquad \text{(mass)} \qquad (3.5)$$

$$u_t + uu_r + p_r/\rho = 0 \qquad \text{(momentum)} \qquad (3.6)$$

$$(p\rho^{-\gamma})_t + u(p\rho^{-\gamma})_r = 0 \qquad \text{(state)} \qquad (3.7)$$

The third of these equations is not quite equivalent to (3.4), since it only expresses the fact that the entropy is constant along the path of an element, and does not imply its constancy throughout. This is a difference from the case of plane waves; another difference from the equations of one-dimensional flow is the additional term $2u\rho/r$ occurring in (3.1) and (3.5), which stands essentially for the spherical attenuation of the wave. This

term of course is very important to the problem.

A complete geometrical description of the disturbance is afforded by the construction of an r,t-diagram, as shown in Fig. 3. Here the solid lines represent the motion of the points of a spherical surface, referred to as a "particle". The most prominent feature in this diagram is a discontinuity, or shock front which propagates through the material at the head of the disturbance. This curve, together with the cavity boundary, defines a region (shaded in the figure) in which the solution to the system of partial differential equations (3.5), (3.7) applies. Certain boundary conditions, to be discussed later, must be satisfied. However, the difficulty of the problem is that, unlike the conventional boundary value problems, here the boundary curves are themselves unknown, and must be found as part of the problem. In fact, the determination of these two curves are the most important part of the problem.

4. The Method of Progressing Waves

The idea of this and similar mathematical methods is to reduce the partial differential equations to ordinary ones. This is accomplished by assuming the specific form for the shock front curve and imbedding it in a one-parameter family of curves. These curves are called "progressing waves". For general details of the method, see [2] p. 419-433. The method was used by R. G. Newton [4] to analyze blast shock problems.

Our "progressing wave" solutions are defined to be of the form,

$$u = t^{\beta}\, \xi\, U(\xi) \qquad (4.1a)$$

$$\text{with } \xi = rt^{-\alpha}$$

$$\rho = t^{\delta}\, D(\xi) \qquad (4.1b)$$

$$p/\rho = t^{\epsilon}\, \xi^{2}\, P(\xi) \qquad (4.1c)$$

where α, β, δ, ϵ are parameters, and U, D, P functions to be determined. By introducing this variable ξ we have defined geometrically a family of surfaces ξ = const. in the r,t-plane, which will play an important role in the analysis. Although these are not the trajectories of the particles of the medium, we shall see that the shock front belongs to this family of surfaces.

We now explore these solutions mathematically by substituting the expressions (4.1) into the equations of motion (3.5)-(3.7), giving respectively,

$$\xi t^{\beta-1}\Big[\beta U - \alpha(\xi U' + U) + t^{\beta-\alpha+1}U(\xi U' + U) + t^{\epsilon-\alpha-\beta+1}(2P + \xi P D'/D + \xi P')\Big] = 0 \qquad (4.2a)$$

$$t^{\delta-1}[(U-\alpha)\xi D' + \delta D + (\xi U' + 3U)D] = 0 \qquad (4.2b)$$

$$t^{\delta+\epsilon-1}\Big\{-\gamma\xi^2 P(\delta D - \alpha\xi D') + \xi^2[(\delta+\epsilon)DP - \alpha(2DP + \xi D'P + \xi DP')] + t^{\beta-\alpha+1}[-\gamma\xi^2 PD' + \xi(2DP + \xi D'P + \xi DP')]\xi U\Big\} = 0 \qquad (4.2c)$$

The sense in these equations is that it is possible to eliminate the explicit factor t by properly choosing the exponents, thereby leaving a system of functions of one independent variable ξ. This is accomplished by letting

$$\epsilon = 2\beta \quad ; \quad \beta = \alpha - 1 \qquad (4.3)$$

so that $t^{\beta - \alpha + 1} = t^{\epsilon - \alpha - \beta + 1} = 1$ and we then have (after also dividing by $\xi t^{\beta - 1}$, $t^{\delta - 1}$, $t^{\delta + \epsilon - 1}$ which are not zero for $t > 0$, and some simplification,)

$$\beta U - \alpha (\xi U' + U) + U(\xi U' + U) + (2P + \xi PD'/D + \xi P') = 0 \quad (4.4a)$$

$$(U - \alpha) \xi D' + \delta D + (\xi U' + 3U)D = 0 \quad (4.4b)$$

$$P' \xi(U - \alpha) + P[2\beta - \delta(\gamma - 1) + 2(U - \alpha)] - (D'/D)P \xi (\gamma - 1)$$
$$(U - \alpha) = 0 \quad (4.4c)$$

We now have a system of ordinary differential equations for the unknown functions $U(\xi)$, $D(\xi)$, $P(\xi)$ and two free parameters α and δ. The substitutions (4.1), which may appear artificial, are thus justified.

We shall now reduce the number of variables further. Solving (4.4b) for $\xi D'/D$ gives

$$\xi D'/D = - (\delta + \xi U' + 3U)/(U - \alpha) \quad (4.5)$$

When this is put into the remaining two equations we obtain the pair,

$$(U - \alpha) (\xi U' + U) + \beta U + P [2 - (\delta + \xi U' + 3U)/(U - \alpha)]$$
$$+ \xi P' = 0 \quad (4.6a)$$

$$- (\gamma - 1) (\delta + \xi U' + 3U) - 2\beta + (\gamma - 1) \delta - 2 (U - \alpha) -$$
$$- (U - \alpha) \xi P'/P = 0 \quad (4.6b)$$

These equations, linear in $\xi U'$ and $\xi P'$ may be simultaneously solved, giving

$$\xi U' = [- U (U -\alpha) (U - 1) + (\delta + 2\beta + 3U \gamma)P]/\Delta \tag{4.7a}$$

$$\xi P' = P \left\{(\gamma - 1)U(U - 1) - (U -\alpha)[(3\gamma - 1)U - 2] + \right.$$

$$\left. + \left(\frac{2\beta - (\gamma - 1)\delta}{U - \alpha} + 2\gamma\right)P \right\} /\Delta \tag{4.7b}$$

where $$\Delta = (U - \alpha)^2 - \gamma P \tag{4.7c}$$

The final step is to obtain by division of (4.7b) by (4.7a) the ordinary differential equation

$$\frac{dP}{dU} = \frac{\xi P'}{\xi U'} = \frac{P [N(U) + P Q (U)]}{R (U) + P S (U)} = \frac{F(U,P)}{G(U,P)} \tag{4.8a}$$

where, after simplification,

$$\begin{aligned} N(U) &= \gamma U(3\alpha - 1 - 2U) + (3 - \alpha) U - 2\alpha \\ Q (U) &= \left\{[2\beta - (\gamma - 1) \delta]/(U - \alpha)\right\} + 2\gamma \\ R (U) &= U(U - \alpha) (1 - U) \\ S (U) &= \delta + 2\beta + 3U\gamma \end{aligned} \tag{4.8b}$$

This is the basic differential equation for progressing waves. After the appropriate solution has been found for $P = P(U)$, the function $\xi = \xi(U)$ is found by a quadrature of (4.7a) and the density function $D(\xi)$, from (4.5).

These progressing wave solutions, as we shall see, provide a sufficiently general mathematical description of an expanding cavity reasonably consistent with the given conditions of initiation of the process. There remains the problem of choosing the two parameters α and δ. For this we have two possibilities of an assumption:

(a) the motion is isentropic

(b) the motion is adiabatic, with constant total energy.

If (a) holds, then from eqs. (3.4) and (4.1),

$$p\rho^{-\gamma} = (t^{\epsilon}\xi^2 P)\,(t^{\delta}D)^{(1-\gamma)} = A$$

or
$$t^{\epsilon + (1-\gamma)\delta}\,\xi^2 P D^{(1-\gamma)} = A$$

requiring, for independence of time, that

$$\epsilon + (1-\gamma)\delta = 0. \tag{4.9}$$

This condition is not, in general, satisfied by a spherical wave. Instead, we have the condition (b), that is, constant total energy. This is a reasonable one for the cavity expansion process, because of its short duration, provided certain secondary effects are neglected. With $\xi = \xi_1$ representing the shock front at a time t, the total energy in the fluid shell (potential + kinetic) at time t is given by

$$E(t) = \int_{r_o}^{r_1} \left(\frac{p}{\gamma-1}\right) 4\pi r^2\,dr + \int_{r_o}^{r_1} \frac{1}{2}\,\rho u^2\, 4\pi r^2\,dr \tag{4.10}$$

where $r_o = \xi_o t^{\alpha}$ is the inner radius of the shell (Fig. 1) and $r_1 = \xi_1 t^{\alpha}$ is the location of the shock front.

The first term arises from the polytropic relation $p = A\rho^{\gamma}$ which has been assumed for the material and the fact that the work done by the material in becoming compressed from an initial volume V_o to a volume V is given by

$$E(V) = \int_{V_o}^{V} pdV = \rho_o V_o \int_{\rho_o}^{\rho} A\rho^{\gamma}\left(-\frac{d\rho}{\rho^2}\right) = -\frac{pV}{\gamma-1} + \text{const.} \tag{4.11}$$

where we have used the relation $\rho V = \rho_o V_o$. Using the substitutions in (4.1) the energy expression becomes

$$E(t) = 4\pi \int_{r_o}^{r_1} (t^{\delta} + \epsilon \frac{P}{\gamma-1} + \frac{1}{2} t^{\delta + 2\beta} U^2)\xi^2 D(\xi) r^2 dr$$

Substituting $r = \xi t^{\alpha}$, $dr = t^{\alpha} d\xi$, since t is constant,

$$E(t) = 4\pi t^{\delta + 5\alpha - 2} \int_{\xi_o}^{\xi_1} (\frac{P}{\gamma-1} + \frac{1}{2} U^2)\, \xi^4 D(\xi)\, d\xi \tag{4.12}$$

Since the integral is independent of t, we make the <u>energy independent of time</u> by satisfying the relation

$$\delta + 5\alpha - 2 = 0 \quad \text{or} \quad \delta = 2 - 5\alpha \tag{4.13}$$

5. Boundary Conditions at Shock Front

We shall narrow down the number of parameters by examining the compatibility of our solution with the basic Rankine-Hugoniot conditions across a shock front. If the undisturbed and disturbed medium parameters are u_o, ρ_o, p_o and u_1, ρ_1, p_1 respectively and the shock wave velocity is C, then these relations are (See [2], p. 123-4),

$$\rho_o (u_o - C) = \rho_1 (u_1 - C) = m \qquad \text{(conservation of mass)} \qquad (5.1a)$$

$$\rho_1 u_1 (u_1 - C) - \rho_o u_o (u_o - C) = p_o - p_1 \qquad \text{(conservation of momentum)} \qquad (5.1b)$$

$$\rho_1 \left(\tfrac{1}{2} u_1^2 + E_1 \right) (u_1 - C) - \rho_o \left(\tfrac{1}{2} u_o^2 + E_o \right) (u_o - C) = p_o u_o - p_1 u_1 \qquad \text{(conservation of energy)} \qquad (5.1c)$$

where $E = \frac{1}{\gamma - 1} \frac{p}{\rho}$ for a polytropic medium.

When the undisturbed state is a medium at rest, with $u_o = 0$, these reduce to

$$\rho_1 (C - u_1) - \rho_o C = 0 \qquad (5.2a)$$

$$\rho_1 u_1 (C - u_1) - (p_1 - p_o) = 0 \qquad (5.2b)$$

$$\rho_1 \left(\tfrac{1}{2} u_1^2 + \frac{1}{\gamma - 1} \frac{p_1}{\rho_1} \right) (C - u_1) - p_1 u_1 = 0 \quad (E_o = 0) \qquad (5.2c)$$

It is useful to have (5.2a) and (5.2b) solved for the velocities, giving

$$u_1 = (p_1 - p_o)/(\rho_o C) \qquad (5.3a)$$

$$C = \sqrt{\frac{\rho_1}{\rho_o}\,\frac{p_1 - p_o}{\rho_1 - \rho_o}} \tag{5.3b}$$

If p is in kilobars, ρ in gm/cc, then u and C will come out in km/sec by the following formulas:

$$u_1 = (p_1 - p_o)/(10\,\rho_o\,C) \tag{5.4a}$$

$$C = \sqrt{\frac{\rho_1}{\rho_o}\,\frac{p_1 - p_o}{10\,(\rho_1 - \rho_o)}} \tag{5.4b}$$

It is useful to have these relations for a polytropic medium

$$u_1 = \sqrt{\frac{2}{\gamma-1}\,\frac{p_1}{\rho_1}\cdot\frac{p_1 - p_o}{p_1 + p_o}} \tag{5.5a}$$

$$C = \frac{1}{1 - \frac{\rho_o}{\rho_1}}\sqrt{\frac{2}{\gamma-1}\,\frac{p_1}{\rho_1}\cdot\frac{p_1 - p_o}{p_1 + p_o}} \tag{5.5b}$$

From (5.3a), with $\mu = \sqrt{(\gamma-1)/(\gamma+1)}$, if p_o is negligible,

$$u_1 = C\,(1 - \mu^2) \tag{5.6a}$$

$$p_1 = \rho_o\,u_1\,C = \rho_o\,C^2\,(1 - \mu^2) \tag{5.6b}$$

$$\rho_1/\rho_o = (\gamma + 1)/(\gamma - 1) = 1/\mu^2 \tag{5.6c}$$

$$c = \sqrt{dp/d\rho} = \sqrt{1 + \mu^2}\,C$$

The last quantity is conveniently referred to as the "sound speed" in shock wave analysis.

These relations apply just as well to a spherical or curved surface as to a plane, since the effect of spherical divergence (the $2u/r$ term) on a finite or sudden jump is of higher order. This may also be shown geometrically by considering an infinitesimal surface element of the shock front. Since $\xi_1 = rt^{-\alpha}$ along the shock front,

$$0 = t^{-\alpha}\, dr - \alpha r t^{-\alpha-1} dt$$

so $c = \frac{dr}{dt} = \alpha r t^{-1} = \alpha \xi_1 t^{\alpha-1}$. From (4.1) and the relations (4.3) with

$c - u_1 = \alpha \xi_1 t^{\alpha-1} - t^{\beta}\, \xi_1 U(\xi_1) = \xi_1 t^{\beta}\, (\alpha - U)$, we obtain

$$t^{\delta+\beta}\, \xi_1 D(\alpha - U) - \rho_o \alpha \xi_1 t^{\beta} = 0 \qquad (5.7a)$$

$$t^{\delta+2\beta}\, \xi_1^2 DU\, (\alpha - U) - t^{\delta+2\beta}\, \xi_1^2 DP = 0 \qquad (5.7b)$$

$$t^{\delta+3\beta}\, D\xi_1^2 \left(\tfrac{1}{2} U^2 + \frac{1}{\gamma-1} P \right) \xi_1\, (\alpha - U) - t^{\delta+3\beta}\, \xi_1^3\, DPU = 0 \qquad (5.7c)$$

We note that the time factor cancels in (5.7b) and (5.7c), so that they are automatically satisfied, but to secure independence of time in (5.7a), it is necessary to make

$$\delta = 0 \qquad (5.7d)$$

With this condition, and the relations (4.3), the assumed form for the progressing wave solutions reduce to

$$u = \frac{r}{t} U(\xi) \qquad p = \left(\frac{r}{t}\right)^2 D(\xi)P(\xi)$$

$$\rho = D(\xi) \qquad \frac{p}{\rho} = \left(\frac{r}{t}\right)^2 P(\xi) \tag{5.8}$$

$$\text{with } \xi = rt^{-\alpha}$$

This solution shows that on the shock front or free surface, where ξ is constant, the physical quantities such as velocity, pressure, density, and wave velocity are constant on the rays r/t = constant. This also dimensionalizes the functions (5.8) correctly, for, with ξ having the dimensions of length per $(\text{time})^{\alpha}$, and

$$\xi = [LT^{-\alpha}] \qquad D(\xi) = [ML^{-3}] \text{ density}$$

$$U(\xi) = [1] \qquad P(\xi) = [1]$$

then u, p, ρ, p/ρ come out correctly to have respectively the dimension of velocity, pressure $(ML^{-1}T^{-2})$, density, and velocity squared. The complete set of exponents is now

$$\alpha = 2/5 \qquad \epsilon = -6/5$$

$$\beta = -3/5 \qquad \delta = 0 \tag{5.9}$$

Initial Conditions

Since $\xi = \xi_1$ on the shock front, we have, just behind it,

$$U(\xi_1) = \alpha(1 - \mu^2) = 2\alpha/(\gamma + 1) \tag{5.10a}$$

$$D(\xi_1) = \rho_o/\mu^2 \tag{5.10b}$$

$$P(\xi_1) = \alpha^2\mu^2 (1 - \mu^2) = 2\alpha^2\mu^2/(\gamma + 1) \tag{5.10c}$$

with $\alpha = 2/5$ or $1/4$ according as the energy or momentum condition holds.

The right side of equations (5.10) give us, for a specified material, a definite point in the P-U plane, through which a single solution curve is determined in general. We may refer to this point as our "initial point", and proceed to draw the solution curve. Note that the constant ξ_1, still undetermined, is not needed for this. We will discuss in Section 10 how this constant may be determined.

6. Equation of State of Aluminum

In Fig. 4 is shown the relationship between pressure and relative density for aluminum in the range between 100 and 400 kilobars. The three numbered data points are taken from Ref. [3] as follows:

24 ST aluminum

$\rho_o = 2.785$ free space density

$c_p = 0.23$ sp. heat at const. pressure

$\frac{1}{V}\left(\frac{\partial V}{\partial t}\right)_p = 69.0 \times 10^{-6}/^{\circ}C$

	P_3	P_2	P_1
Pressure (kb):	335.8	222.7	153.5
Rel. volume V/V_o:	0.7874	0.8333	0.8696
Shock wave velocity U_s: (km/sec)	7.531	6.927	6.500
Free surface velocity: (km/sec)	3.230	2.319	1.700

These points are plotted on logarithmic paper in Fig. 4, and a straight-line fit through these points is possible, leading to the polytropic-type relation

$$p\left(\frac{\rho}{\rho_o}\right)^{-7.60} = 52.7 \qquad 100 \text{ kb} < p < 400 \text{ kb} \qquad (6.1)$$

where p is in kilobars.

A few points are shown beyond the 400 kb range based on additional data taken from [3]. Here there is a slight but consistent departure from the equation of state (6.1). However under the conditions of our explosion the range of pressures do not exceed 400 lb.

Below about 100 kb we have a transition to elastic-plastic or elastic behavior. The nature of this transition is considerably uncertain. We may also note that, unlike gases, the value of γ is very high, i.e., relatively small density changes occur under very high pressures.

The polytropic-type equation of state is a very convenient one to use for metals provided the pressure range is restricted, such as in (6.1). It has the advantage that the progressing wave procedure in eqs. (4.2) can be carried through. However, such an equation of state must always be modified at low pressures since the density of a solid does not tend to zero with the pressure. Other equations of state have been used, e.g. Sedov in [11], and Stanukovich [15], have used the formula

$$p = A\left[(\rho/\rho_o)^{\gamma} - 1\right] \qquad (6.2)$$

For aluminum, the values $A = 187$, $\gamma = 4.27$, $\rho_o = 2.7$ provide a good fit to the data points of Fig. 4.

Further discussion of equations of state for solids is given by Huang [14].

7. The Explosion Process

A physical description of the explosion process taking place in the expanding inner cavity is naturally very important to our problem as this provides the pressure forcing function required to expand the metal. Although much is known about the unconfined explosion, the main difficulty of our problem is that the gas is confined by the metal during the process. Our knowledge of the effect of this confinement, at least for the explosives used in the experimental study, is limited to empirical factors.

A condensed explosive such as "Pentolite" is converted, upon explosion, into a gas at high temperature across a rapidly moving discontinuous front, referred to as a detonation wave. Behind this front the chemical composition changes until a number of stable end-products are reached. The detonation process in Pentolite has been analyzed in detail by Shear [5], [6] using the hydrodynamic theory of detonation, and an equation of state worked out giving the pressure-density relationship behind the detonation front. This is shown in Fig. 5. It may be assumed that the gas expands isentropically.

The detonation values for Pentolite are, from [6]:

Loading density of solid:	$\rho_o = 1.655$ gm/cc
Initial explosion pressure:	$P_1 = 231.250$ kilobars
Explosion temperature:	$T_1 = 3367.7^\circ$ K
Detonation velocity:	$D = 7807$ m/sec

The equation of state curve of Fig. 5 is not fitted too well for the entire range by a polytropic equation (straight line). However, over a small part of the range of pressures, we may refer to the slope γ as the "local" adiabatic exponent. This varies from $\gamma = 3.29$ at the front down to $\gamma = 1.32$.

For rough approximate purposes the high value of γ may be used for pressures down to 100 kb.

These results are in very good agreement with experiments for unconfined explosions, or explosions in air. However, there is still lacking a detailed study of the interaction between the expanding gaseous products of the explosive and the metal surface confining it. The expansion of the gas is considerably complicated by the detonation wave reflecting off the metal boundary, probably many times. Thus the loading pressure P_r against the metal will be higher than the detonation pressures P_s behind the front, as exhibited in Fig. 5. While the latter are accurately known, the loading pressures are uncertain. Doring, in [10], p. 226, formula (4), gives data of this type for other materials than Pentolite. With these data as a guide an estimate of 26% increase in pressure due to confinement is tentatively suggested, i.e.

$$P_r = 1.26\, P_s$$

Thus, for a detonation pressure of 231 kb,

$$P_r = 292 \text{ kb}$$

The same reference also furnishes the value $u = 1400$ m/sec for the initial particle velocity in aluminum.

In the early stages of the explosion process (up to approximately 2 microsec) the actual value may be substantially higher.

It may reasonably be assumed that this factor remains constant at different pressures, so that the curve of Fig. 5 is just shifted up a constant amount. Until more detailed studies are available, this would be the easiest way to extrapolate the confinement factor down to lower pressures.

The analysis of the confinement problem requires a model for the density variation with radius of the exploding gas. Thus, the simplest model would be a gas in equilibrium, and hence at uniform density, in the cavity, as shown by curve (a), Fig. 6. Given the pressure-density relation, the pressure against the metal would be easily calculated from the instantaneous cavity radius $R(t)$ according to the relation $\rho = \rho_o (R_o/R)^3$. A more realistic distribution of non-uniform density is shown in (b), which puts the maximum density and pressure at the interface. It assumes the detonation front remains in contact with the interface and therefore the Hugoniot relation of Fig. 5 may be used. However, further assumptions are required to relate the density to radius $R(t)$ or to the time t itself. The third model (c), which is only sketched, is a further refinement in that it accounts for the reflection of the detonation front off the interface.

The equilibrium model (a) can only become accurate during the latter phase of the cavity expansion, after several reflections of the detonation wave. Fig. 12 compares gas pressures on this model with that of the solid. They are too low at first, and too high later. The critical time occurs at 2.5 microseconds. The probably state of affairs is that the detonation wave remains in contact with the metal for this period of time and then releases the pressure.

8. The P, U- Diagram

Using the condition of constant energy, the 2/5-power law holds, and the differential equation (4.8) for progressing waves may be solved. This was done numerically by means of Program I given in the Appendix. A family of integral curves in the diagram are shown in Fig. 7. All of them issue from the singular point A enclosed in a rectangle on the diagram, and which is located by equating

$$F(U, P) = 0 \quad , \quad G(U,P) = 0$$

in (4.8). For our set of constants this point is

$$U_o = 0.0916 \quad , \quad P_o = 0.02884 \tag{8.1}$$

A more detailed analysis of the singular points is given in the Appendix. The immediate neighborhood of this point is shown plotted in Fig. 8. It can be seen that all the curves come out of this point along a common tangent, and the point is labelled an "unstable nodal point" or simply, a "source". The point $U = 0$, $P = 0$ is a stable nodal point, or "sink", and the point

$$P_o = 0 \quad , \quad U_o = 0.4$$

is a saddle point. (See Appendix C.) The solution curve for the physical problem starts close to the source, then runs over very close to the saddle point. There is a unique curve (marked C in Figs. 7 and 8) which actually runs into the saddle, as shown in Appendix C. The accuracy of the computations is not sufficient to distinguish whether our solution actually coincides with C or not.

The "source" point itself represents physically an infinite shock strength, as sketched in Fig. 9(b). Here the pressure and density just behind the shock front are infinite (with a finite total impulse, however) and the particle velocity is equal to the shock wave velocity. This type of condition arises in stress-wave propagation problems as well, in the form of a δ-function at the wave-front. See [16]. It is a consequence of the assumed instantaneous (i.e. step) loading of the material. With such a loading we must start the propagation of either a zone of infinite pressure if the velocity is finite, or our front must start out with an infinite velocity.

The end-point of the solution curve C at $U = \alpha$, $P = 0$ provides a very reasonable physical condition of asymptotic character. For, if we consider any point A in the r,t-plane, Fig. 11, the "particles" must cross the family of curves

$$r = \xi t^{\alpha} \tag{8.2}$$

(shown dotted) from left to right, since we have compression shock. Thus the particle curve (solid) has a lower slope at A than that of the dotted curve:

$$u = \frac{r}{t} U(\xi) < \frac{\delta r}{\delta t} = 0.4 \frac{r}{t}$$

This condition is always satisfied since all the solution curves in the U,P-plane coming out of the unstable nodal point lie to the left of the vertical line $U = 0.4$. However, for the curve C $u \to 0.4\ r/t$ as $t \to \infty$, i.e. the particle curve is asymptotic to (8.2). The $P = P(U)$ curves which end in $U = 0$, $P = 0$ give particle curves which cross all the curves of (8.2).

9. The Radius-Time r,t-Diagram

Figs. 10 and 11 show an r,t-diagram plotted for an initial cavity radius of 1.698 cm. Pressures in kilobars are also shown on Fig. 10. This figure gives much more detail of the early phase of the expansion up to $t = 2.5$ microsec. from its start at $t = 0.9$ μ sec. In this elapsed time of 1.6 μ sec the inner cavity has only grown to 1.86 cm, which is only 13% of its ultimate change However, the pressure has already fallen considerably. At the cavity surface it is down to 50 kb.

We also note that the shock velocity at point labelled P on the diagram is equal to the known elastic wave velocity of the material. Beyond

this point the 2/5-power law for the shock front starts to deviate from this velocity. Such a condition represents a discrepancy of the progressing wave method from this point on which is inevitable because of the equation of state used.

Figs. 12, 13, and 14 show how the pressure, particle velocity and density decay with time at the inner cavity surface. We note that $\rho = \rho_o$ occurs for $t = 2.5\ \mu$ sec. Of course, we may not conclude that ρ becomes less than the free space density because the equation of state (6.1) no longer applies.

10. Results

TABLE 1

Variation of physical quantities along solution curve and cavity surface

T	U	P	ξ	D	E	R(2)
sec x 10^{-6}				gm/cc	ergs x 10^{12}	cm
.8684	.09302	.02856	451.28(1)	3.5182	-0.0	1.698
.9539	.09312	.02854	438.45	3.4282	-.188	1.713
1.062	.09324	.02852	424.25	3.3282	-.368	1.730
1.186	.09337	.02844	410.10	3.2282	-.520	1.748
1.329	.09352	.02846	396.02	3.1282	-.648	1.767
1.495	.09369	.02843	381.99	3.0282	-.755	1.786
1.688	.09389	.02840	368.02	2.9282	-.844	1.807
1.939	.09411	.02836	354.12	2.8282	-.918	1.828
2.181	.09436	.02832	340.29	2.7282(3)	-.979	1.851
2.496	.09466	.02827	326.52	2.6282	-1.029	1.874
2.872	.09500	.02821	312.83	2.5282	-1.069	1.900
3.323	.09539	.02815	299.2194	2.4282	-1.101	1.926
3.868	.09586	.02807	285.69	2.3282	-1.127	1.954
4.533	.09641	.02799	272.24	2.22818	-1.148	1.984
5.350	.09707	.02789	258.89	2.1282	-1.164	2.016
6.364	.09787	.02777	245.63	2.0282	-1.176	2.050
7.636	.09884	.02764	232.48	1.9282	-1.186	2.087
9.252	.10003	.02749	219.43	1.8282	-1.193	2.127
11.33	.10152	.02731	206.51	1.7282	-1.198	2.171
14.04	.10341	.02710	193.71	1.6282	-1.202	2.219
17.65	.10585	.02686	181.05	1.5282	-1.205	2.272
22.52	.10904	.02659	168.55	1.42818	-1.207	2.332
29.28	.11331	.02628	156.21	1.3282	-1.209	2.401
38.91	.11914	.02593	144.08	1.2282	-1.210	2.481
53.07	.12728	.02555	132.17	1.1282	-1.211	2.577
74.76	.13883	.02513	120.56	1.0282	-1.211	2.696
109.5	.15536	.02462	109.38	.9282	-1.212	2.849
168.3	.17866	.02384	98.85	.8282	-1.212	3.058
273.2	.21002	.02241	89.36	.7282	-1.212	3.355
470.8	.24867	.01974	81.30	.6282	-1.212	3.795
865.8	.29068	.01550	74.96	.5282	-1.212	4.465
1717	.32972	.01012	70.40	.4282	-1.212	5.514
3681	.35941	.00478	67.43	.3282	-1.212	6.968
7404	.37363	.00098	65.87	.2282	-1.212	9.257
8357	.36027	.00001	65.67	.1282	-1.212	9.687

(1) See below

(2) Cavity radius

(3) Free-space density $\rho = \rho_o$

From eq. (4.5), it can be seen that the ξ-function admits of an arbitrary multiplicative constant. This constant is determined from the known required density of the material behind the shock front given by the Rankine-Hugoniot conditions. This is given by (5.6c). From the equation of state (6.1),

$$\rho = 3.5182$$

$$p = 384 \text{ kb}$$

Then, from (5.10b) and (5.10c),

$$D = 3.5182 \quad , \quad P = .02856.$$

For an initial cavity radius of $r = 1.698$ cm, eq. (5.8) gives

$$t = r(DP/p)^{\frac{1}{2}} = 0.868 \text{ microseconds.}$$

This is the value which must be used as the starting time of the cavity motion in order to put the shock front at the given radius. We finally must have

$$\xi = \xi_1 = rt^{-\alpha} = (1.698)\ (.868 \times 10^{-6})^{-.4} = 451.28.$$

11. Energy Considerations

In the theory of progressing waves, an assumption of constant energy was made (see eq. (4.12) in order to provide the condition (4.13) for determining α and with it, all the other exponents. The energy integral (4.12) is extended between two points, one of which is located on the shock front $\xi = \text{const.} = \xi_1$ and a lower value $\xi = \xi_0$. The integral path, such as BC in Fig. 3, may be arbitrarily chosen, so long as it terminates on these two curves.

The energy in the disturbed part of the solid will, however, change with time because its lower boundary, the cavity surface, is not one of the family of ξ-curves. Thus the energy values in Table 1 represent an integration of the expression in (4.12) taken along the cavity surface curve. If we extend this integration far enough (say to 100 microsec) so that point D practically coincides with point C, the values in the table become asymptotically constant, and we have

$$E = \int_A^C = \int_A^B + \int_B^C = 0 + \int_B^D = - \int_{\xi_0}^{\xi_1}$$

From Table A we see that the energy does tend to a constant and we have just shown that this limit is the value of the energy integral (4.12).

$$E = 1.212 \times 10^{12} \text{ ergs} \qquad (11.1)$$

If we now suppose that all (or any known fractional part) of the energy given up by the explosive is transmitted into the solid, then the shock process could be terminated when the energy reaches the amount available. It is not possible to determine a precise point of time because of the asymptotic way in which the energy increases. It is seen, however, that E reaches 90% of its ultimate value in 3 microseconds, which is a very short time compared with the expansion process.

The post-shock expansion presumably must take place under constant energy conditions for a "long" period of time, until it is dissipated by viscosity of the flow, elastic waves, and other side effects.

For energy available in the explosive, Shear [6] gives the value

$$E_{Total} = 1.152 \text{ k cal/g}$$

which, for our explosive weight of 0.07 lb, gives

$$E_{Total} = 1.26 \times 10^{12} \text{ ergs}$$

Our calculated asymptotic value (11.1) from the progressing wave integration comes to 96% of this. Thus we have here an independent comparison to check the theory.

12. Summary and Conclusions

In this paper we have attempted to study the cavity formation process in the metal by determining how the important physical variables of cavity radius, velocity, pressure, and density vary with time and position near the cavity. The most prominent general feature of the whole process is the short time of the "shock" regime as compared with the total time of the expansion. One general criterion of the end of the shock is when the supersonic velocity of the shock front drops to sonic, i.e., at the point P of Fig. 10, where the slope attains the value for elastic disturbances in the material. The progressing wave curve cannot be used beyond this point since it would give a subsonic shock velocity. This situation has occurred after 0.5 microsec.

We note that the highest pressures and densities in the metal are located just behind the shock front, and trail off with decreasing radius to minimum values at the cavity boundary. We note that the equation of state (6.1) which has been used for the calculations has a lower limit of $p = 100$ kb. This could also be used as a criterion for shock termination (point D, Fig. 10). It is reached in 0.7 μ sec. These conditions thus determine a roughly parallelogram shaped region ODPE in the r,t-plane for the validity of the progressing wave region. Note that the cavity has only

expanded 0.1 cm during this period, which is 1/30 of the total observed increase in radius. We are thus justified in referring to the shock process as impulsive, i.e., the later stages of the process are insensitive to many features of the shock part. Hence the progressing wave method of integration remains valid for the analysis of the shock zone.

The asymptotic characteristics of the progressing waves are thus not of direct physical interest since they do not apply to the problem beyond the region described above. The expansion zone, headed by a wave travelling with the dilatational wave velocity goes on for at least 100 μ seconds, during most of which the metal continues to move by fluid or plastic flow.

The final cavity radius attained is of great interest to the general problem as this value is directly observable on the specimens after blast. In principle the prediction of this radius should afford a test of any theory, but the matter is not so direct as this, since several theories are involved. It is now evident that the cavity formation process is complicated. It starts under one theory (in which the state of the metal is fairly well established) but terminates in a different state of the material, about which information is almost completely lacking. Several mechanisms have been suggested for terminating the cavity expansion:

(1) An energy-level criterion

(2) A temperature criterion

(3) A yield-point criterion

Criteria such as (2) or (3) are tempting because they tend to provide fairly definite marks as to when the material "freezes", either when a given temperature, or a given pressure is reached. However, knowledge of materials is still too incomplete to solve this problem. The total energy of the moving material stops increasing after the expansion phase has begun,

so there is no change in energy. Furthermore, any quantitative use of energy balances would require careful accounting of all the energy losses as well. A discussion of some of these energy questions was given in the previous section.

Summary

We summarize by noting that the following four phenomena are coincident in time:

1. The shock-wave becomes sonic

2. The pressure at the cavity surface drops to less than 100 kb

3. The total energy in the disturbed material reaches 90% of its maximum and then levels off asymptotically.

4. The average gas pressure in the cavity (uniform model) equals that in the metal.

All of these occur close to 2 microseconds after initiation of the explosion. This delineates a fairly definite time point of changeover of conditions. Up to this time ($t \cong 2.5$ microsec. for the conditions of this report) we may say the effects of shock predominate. The progressing wave method furnishes an accurate theory for this regime. After this time a relatively long expansion period occurs at constant energy until ultimately terminated by degradation processes.

13. Acknowledgement

The work of this paper was sponsored by the Ballistic Research Laboratories, Aberdeen Proving Ground. Their support is gratefully acknowledged.

Acknowledgement is also due to R. L. Shear and O. T. Johnson of the B.R.L. staff for many helpful discussions.

APPENDIX - Numerical Programs

A. Calculation for the P,U-diagram

The differential equation (4.8a) was solved numerically on the IBM 7074 at The Pennsylvania State University using a FORTRAN program reproduced below. A list of the variables in the notation of this paper, together with their symbols on the program is given in Table A. The method used was first to parametrize the curves $P = P(U)$ in terms of arc length s, so as to avoid difficulties when the solution curves have vertical tangents. Thus, the element of arc of the curve is given by

$$ds = \sqrt{1 + (dP/dU)^2}\, dU \tag{A.1}$$

Substituting the expression (3.8a) in this we have

$$\frac{ds}{\sqrt{P^2(N + PQ)^2 + (R + PS)^2}}\,(R + PS) = dU \tag{A.2}$$

$$\frac{ds}{\sqrt{P^2(N + PQ)^2 + (R + PS)^2}}\,P(N + PQ) = dP \tag{A.3}$$

The square root in the denominator is never zero except at the singular points of the differential equation. To calculate the special curve ⓒ of Fig. 7 efficiently advantage was taken of the fact that the source point in the rectangle becomes a "sink" i e a stable node if the direction of integration on each curve is reversed. Accordingly, a starting point B was chosen near the saddle point, with the coordinates

$$U = 0.3990 \qquad P = 0.0002$$

(using the known slope $m = -0.2$, see Appendix C, eq. (C.2) and the program I was run with $DS = -0.001$. The computed curve then ended very accurately at the original source point.

B. R,T-diagram Program

This program is independent of the Program A, but actually incorporates the calculations of A within itself. It calculates the "particle trajectories" directly from the initial conditions. It also calculates the corresponding $P(U)$ curve. For this program it was found best to use the density D as independent variable, incremented at uniform steps. This is because density is the most sensitive variable in the portion of the curves of physical interest. (See Table 1).

TABLE A - Program Symbol Table for P,U-Diagram

Program Symbol	Our Notation or Name	Eq. Ref.	Mode
A	α		FLT
B	β		"
C	δ		"
G	γ		"
U	U		"
P	P		"
DS	ds		"
X	ξ		"
D	ρ		"
IMAX	num. of iterations		FIX
EP	potential energy	(8.3)	FLT
EK	kinetic energy	(8.3)	"
E	E(t)	(8.3)	"
FN	N(U)	(3.8b)	"
FQ	Q(U)	"	"
FR	R(U)	"	"
FS	S(U)	"	"
FT	P(N+PQ)	(3.8a)	"
FW	R+PS	"	"
FX	$ds/\sqrt{P^2(N+PQ)^2+(R+PS)^2}$	(A.2)	"
DP	dP	"	"
DU	dU	(A.3)	"
FY	$(U-\alpha)^2-\gamma P$	(6.7c)	"
DX	$d\xi$	(6.7a)	"
DD	$d\rho$	(6.5)	"
PD	$P\rho$		"
DEP		(8.3)	"
DEK		"	"

TABLE B - Additional Symbols for R-T Diagram

(See also Table A)

Program Symbol or Statement	Our Notation or Name	Eq. Ref.	Mode
DO	ρ_o		FLT
R	R		"
St. 47	Initial U	(11.3a)	"
St. 48	Initial P	(11.3c)	"
St. 54	Initial ρ	(11.3b)	"
EX	$1/\alpha$		"
T	t		"
V	u		"
PRES	p		"
DT	dt		"

C. Singular Points of the P,U-Plane

The differential equation (3.8a)

$$\frac{dP}{dU} = \frac{P[N(U) + PQ(U)]}{R(U) + PS(U)}$$

is said to have a singular point whenever $\frac{dP}{dU} = \frac{0}{0}$. Using the expressions (3.8b), this condition occurs if

(S1) $P = 0, \quad U = 0$

(S2) $P = 0, \quad U = \alpha$

(S3) $P = 0, \quad U = 1$

and where

(S4) $$\frac{N(U)}{Q(U)} = \frac{R(U)}{S(U)} = P$$

This condition leads to the cubic equation

$$A_3U^3 + A_2U^2 + A_1U + A_o = 0$$

where

$$A_3 = 2\gamma\,(1 - 3\gamma)$$

$$A_2 = 3\gamma^2(3\alpha - 1) + \gamma\,(7 - 5\alpha) - \gamma(3\delta + 4\beta) + \delta + 2\beta$$

$$A_1 = \gamma(3\alpha\delta + 6\alpha\beta - 2\beta - 4\alpha) + (2 - \alpha)\,(\delta + 2\beta)$$

$$A_o = -2\alpha\,(\delta + 2\beta)$$

For the particular numerical constants given by (5.9) and $\gamma = 7.6$, the point S4 is given by

$$P = 0.02884\ , \quad U = 0.0916$$

For the given constants and $\gamma = 7.6$ for aluminum, the remaining roots of the cubic are imaginary.

Near any isolated singular point (U_o, P_o) we may approximate the differential equation by a linear fractional expression of the form

$$\frac{dP}{dU} \sim \frac{a\,x + by}{c\,x + dy}$$

where $x = U - U_o$, $y = P - P_o$. See Stoker [13], p. 36-45, where tests are given for determining the type of singular point. A summary of the results is as follows:

Singular Point	Coefficients	Classification
$U_o = 0,\ P_o = 0$	$a = 0,\ b = -2\alpha$ $c = -\alpha,\ \alpha = 2\beta$	Stable Node
$U_o = \alpha,\ P_o = 0$	(see below)	Saddle Point
$U_o = 1.0,\ P_o = 0$	$a = 0,\ b = \frac{2\beta}{\alpha-1} + 2\gamma$ $c = \alpha-1,\ d = 3\gamma + 2\beta$	Stable Node
$U_o = .0916,\ P_o = .02884$		Unstable Node

Since the point $U_o = \alpha,\ P_o = 0$ was of special importance (end-point of the solution curve) it was examined directly. Near $U = \alpha$ we have the power-series expansion,

$$P = P_o + \left(\frac{dP}{dU}\right)_{U=\alpha} (U - \alpha) + \ldots \qquad (C.1)$$

Dividing both numerator and denominator in the differential equation (4.8) by $U - \alpha$ and putting

$$m = P/(U - \alpha) \qquad (C.2)$$

we may write

$$\frac{dP}{dU} = m \frac{[N(U) + m\,(2\beta + 2\gamma(U - \alpha)]}{U(1 - U) + (2\beta + 3U\gamma)m} \qquad (C.3)$$

We now inquire whether a solution curve can approach the point $U = \alpha$ with a definite limiting slope (i.e. be locally a straight-line). Letting $U \to \alpha$ in (C.3) putting this expression in (C.1), and dividing by $(U - \alpha)$ we obtain the equation for m:

$$m = m \frac{\alpha(\alpha - 1)(\gamma - 1) + 2\beta\, m}{\alpha\,(1 - \alpha) + m(2\beta + 3\gamma\alpha)}$$

This has the following three solutions:

1) $m = \infty$

2) $m = 0$

3) $m = (\alpha - 1)/3$ for $\beta = \alpha - 1$

Thus there are three solution curves which pass through the point. The first two are the straight lines $U = \alpha$ and $P = 0$ respectively, which are singular solutions to the differential equation. The remaining slope is $m = -0.2$ for $\alpha = 0.4$. This is the limiting slope of the solution curve (c) of Fig. 7. In the same figure, all the solution curves between (c) and the horizontal line $P = 0$ end up at the origin, while those between (c) and the vertical line $U = \alpha$, go to infinity asymptotic to the latter.

REFERENCES

1. Davids, N. and Huang, Y. K., "Shock Waves in Solid Craters", J. Aerospace Sci. 29-5, May 1962, pp. 550-557.

2. Courant, R. and Friedrichs, K., "Supersonic Flow and Shock Waves", Interscience Publishers, 1948.

3. Walsh, John M., Rice, Melvin H., McQueen, Robert G., Yarger, Frederick L., "Shock-Wave Compressions of Twenty-Seven Metals," Phys. Review 108, No. 2, p. 196-216.

4. Newton, R. G., "A Progressing-Wave Approach to the Theory of Blast Shock", J. Appl. Mchs., Sept. 1952, p. 257.

5. Shear, R. E. and McCane, P., "Normally-Reflected Shock Front Parameters", BRL Report 1273, 1960.

6. Shear, R. E., "Detonation Properties of Pentolite", BRL Report 1159, 1961.

7. Goodman, H. J., "Compiled Free-Air Blast Data on Bare Spherical Pentolite", BRL Report 1092, 1960.

8. Makino, R. C. and Shear, R. E., "Unsteady Spherical Flow Behind a Known Shock Line", BRL Report 1154, 1961.

9. Lawton, H. and Skidmore, I. C., "Hugoniot Curves for Inert Solids and Condensed Explosives".

10. Doring, W. and Burkhart, G., "Beitrage zur Theorie der Detonation", Berlin, 1939.

11. Sedov, L. I., "Similarity and Dimensional Methods in Mechanics", Translation by Morris Friedman from 4th Russian Ed., Academic Press, 1959.

12. Hopkins, H. G., "Dynamic Expansion of Spherical Cavities in Metals", Progress in Solid Mechanics I, Sneddon and Hill, North Holland, 1960.

13. Stoker, J. J., "Non-Linear Vibrations", Interscience, 1950.

14. Huang, Y. K., "Shock Waves in Hypervelocity Impact of Metals", September 1962, to be published.

15. Stanukovich, K. P., "Unsteady Motion of Continuous Media", London, Pergamon Press, 1960.

16. Davids, N., "Transient Analysis of Stress Wave Penetration in Plates", J. Appl. Mech. 26E, No. 4, December 1959, pp. 651-660.

```
      COMPILE   RUN  FORTRAN
C      BRL-PENN STATE PROJ BLAST WAVES
C      P-U DIAGRAM PROGRAM
C      DAVIDS-CALVIT
       DIMENSION IDENT(8)
    1  READ 800,A,B,C,G,IDENT
  800  FORMAT(4F10.0,8A5)
       IF(A)2,30,2
    2  READ 801,U,P,DS,X,D,IMAX
  801  FORMAT(5F10.0,I10)
  200  READ 807,EP,EK,E
  807  FORMAT(3F10.0)
       PRINT 805,IDENT
  805  FORMAT(1H1,5X,31HBRL-PENN STATE PROJ BLAST WAVES,4X,8A5)
       PRINT 806
  806  FORMAT(1H0,1HI,8X,1HU,9X,1HP,9X,1HX,9X,1HD,14X,2HEP,
     113X,2HEK,13X,1HE,9X,2HPD)
    3  DO 26I=1,IMAX
    4  FN=G*U*(3.0*A-1.0-2.0*U)+(3.0-A)*U-2.0*A
    5  FQ=(2.0*B-(G-1.0)*C)/(U-A)+2.0*G
    6  FR=U*(U-A)*(1.0-U)
    7  FS=C+2.0*B+3.0*U*G
    8  FT=P*(FN+P*FQ)
    9  FW=FR+P*FS
   10  FX=DS/SQRTF(FT*FT+FW*FW)
   11  DP=FT*FX
   12  DU=FW*FX
   13  FY=(U-A)*(U-A)-G*P
   14  DX=X*FY*FX
   15  DD=-D*(FW+3.0*U*FY)*FX/(U-A)
       PD=P*D
   16  PRINT 803,I,U,P,X,D,EP,EK,E,PD
  803  FORMAT(1H ,I3,4F10.5,3F15.7,1F10.5)
   17  U=U+DU
   18  IF(U)27,27,19
   19  P=P+DP
   20  X=X+DX
   21  D=D+DD
   22  DEP=4.0*3.141593*P*D*(X**4)*DX/(G-1.0)
   23  DEK=4.0*3.141593*(U*U)*D*(X**4)*DX/2.0
   24  EP=EP+DEP
   25  EK=EK+DEK
   26  E=EP+EK
   27  GO TO 1
   30  STOP
   31  END
```

```
      COMPILE   RUN  FORTRAN
C      BRL-PENN STATE PROJ BLAST WAVES
C      R-T CALCULATION PROGRAM
C      DAVIDS-CALVIT
   53 DIMENSION IDENT(6),JDENT(8)
    1 READ 800,A,B,C,G,DO,IDENT
  800 FORMAT(5F10.0,6A5)
    2 READ 809,X,R,DD,IMAX,JDENT
  809 FORMAT(1F10.0,2F10.0,I10,8A5)
   43 IF(IMAX)30,30,44
   44 PRINT 805
  805 FORMAT(1H1,5X,31HBRL-PENN STATE PROJ BLAST WAVES)
   45 PRINT 810,A,B,C,G,DO,IDENT
  810 FORMAT(1H0,5X,5F15.5,5X,6A5)
   46 PRINT 813,X,R,DD,IMAX,JDENT
  813 FORMAT(1H0,5X,3F15.5,I10,5X,8A5)
   47 U=A*(1.0-(G-1.0)/(G+1.0))
   48 P=(A*A*(G-1.0)/(G+1.0))*(1.0-(G-1.0)/(G+1.0))
   54 D=(G+1.0)/(G-1.0)*DO
   49 EP=0
   50 EK=0
   51 E=0
   52 PRINT 806
  806 FORMAT(1H0,1X,1HI,7X,1HT,11X,1HR,12X,1HV,11X,7HPRES KB,8X,1HD,11X,
     11HU,11X,1HP,11X,1HX,12X,1HE)
    3 DO 260 I=1,IMAX
    4 FN=G*U*(3.0*A-1.0-2.0*U)+(3.0-A)*U-2.0*A
    5 FQ=(2.0*B-(G-1.0)*C)/(U-A)+2.0*G
    6 FR=U*(U-A)*(1.0-U)
    7 FS=C+2.0*B+3.0*U*G
    8 FT=P*(FN+P*FQ)
    9 FW=FR+P*FS
   13 FY=(U-A)*(U-A)-G*P
  900 FX=-DD*(U-A)/(D*(FW+3.0*U*FY))
   11 DP=FT*FX
   12 DU=FW*FX
   33 EX=1.0/A
  330 T=(R/X)**EX
   14 DX=X*FY*FX
   34 V=R*U/T
   37 PRES=(R/T)**2*P*D*(10.0**(-9))
  160 PRINT 808,I,T,R,V,PRES,D,U,P,X,E
  808 FORMAT(1H ,I3,1E12.4,1F12.7,1E14.5,1F14.5,4F12.5,1E15.5)
  340 DT=DX/((-A/T+V/R)*X)
   19 IF(P)27,35,35
   35 T=T+DT
   36 R=R+V*DT
   17 U=U+DU
   18 P=P+DP
   20 X=X+DX
   21 D=D+DD
   22 DEP=4.0*3.141593*P*D*(X**4)*DX/(G-1.0)
   23 DEK=4.0*3.141593*(U*U)*D*(X**4)*DX/2.0
   24 EP=EP+DEP
   25 EK=EK+DEK
   26 E=EP+EK
  260 CONTINUE
   27 GO TO 2
   30 STOP
   31 END
```

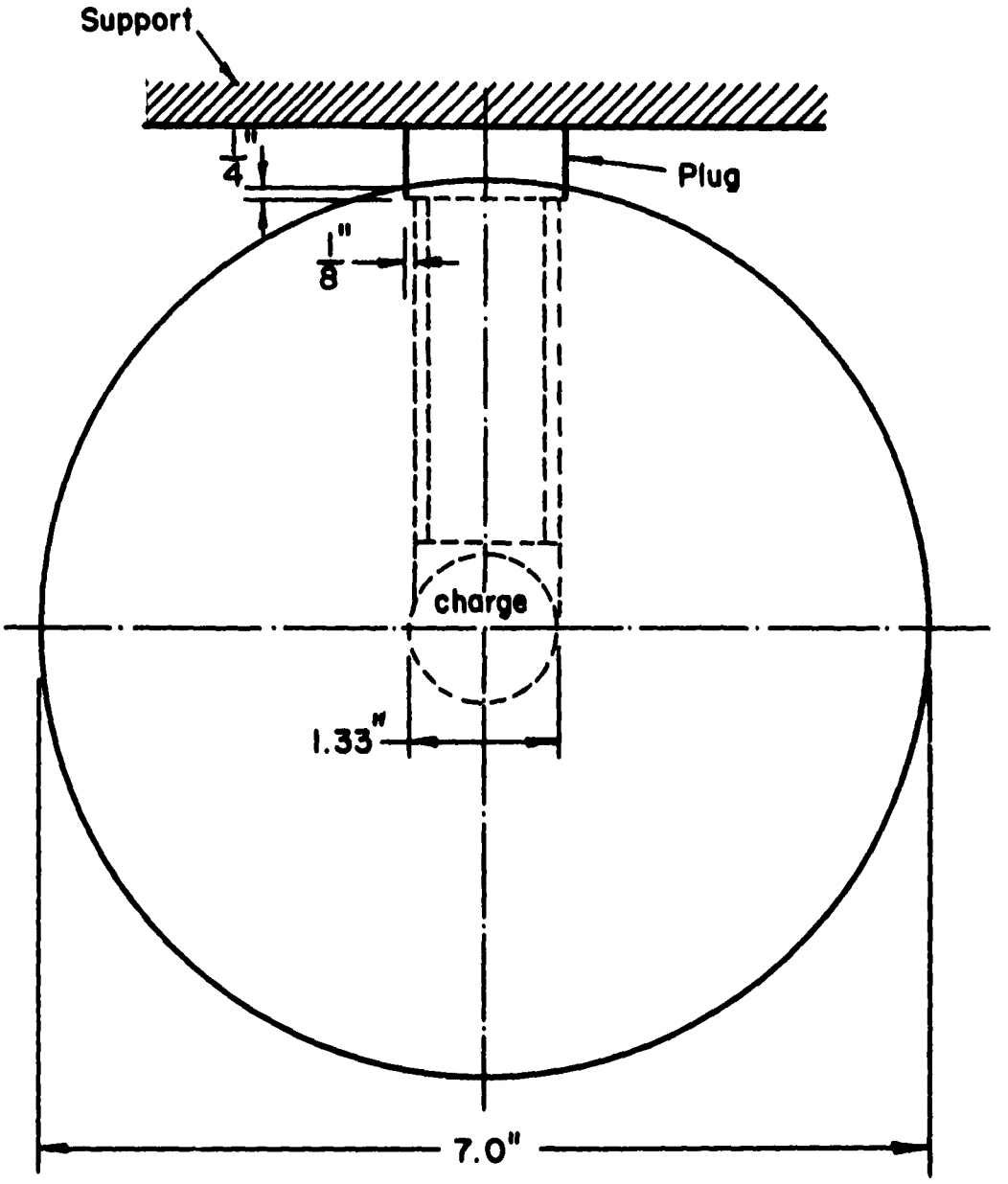

FIG. 1 – ALUMINUM SPHERE – PRE SHOT

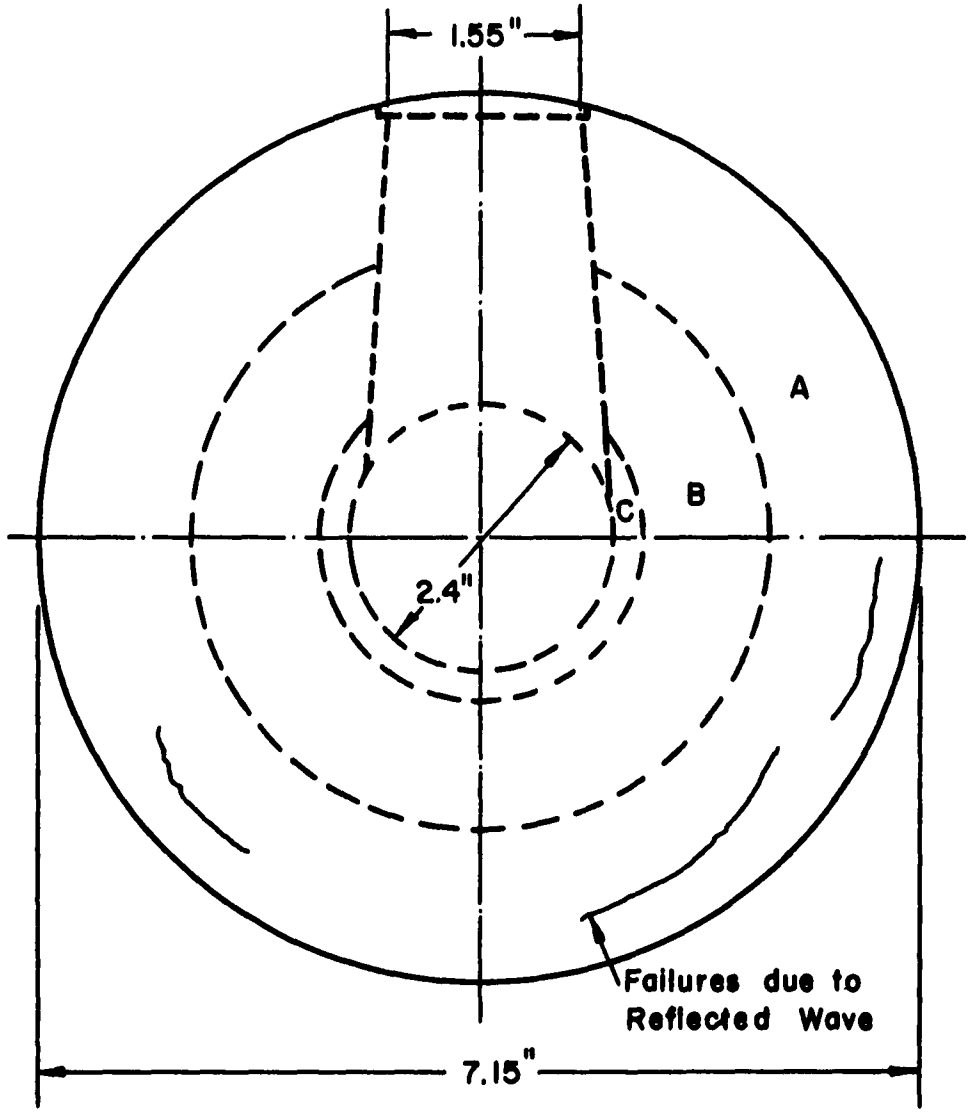

Zone A – No damage, other than that of reflected wave

Zone B – Heavily damaged

Zone C – "Fluid" zone

Note – Dimensions are approximate

FIG. 2 – ALUMINUM SPHERE – POST SHOT.

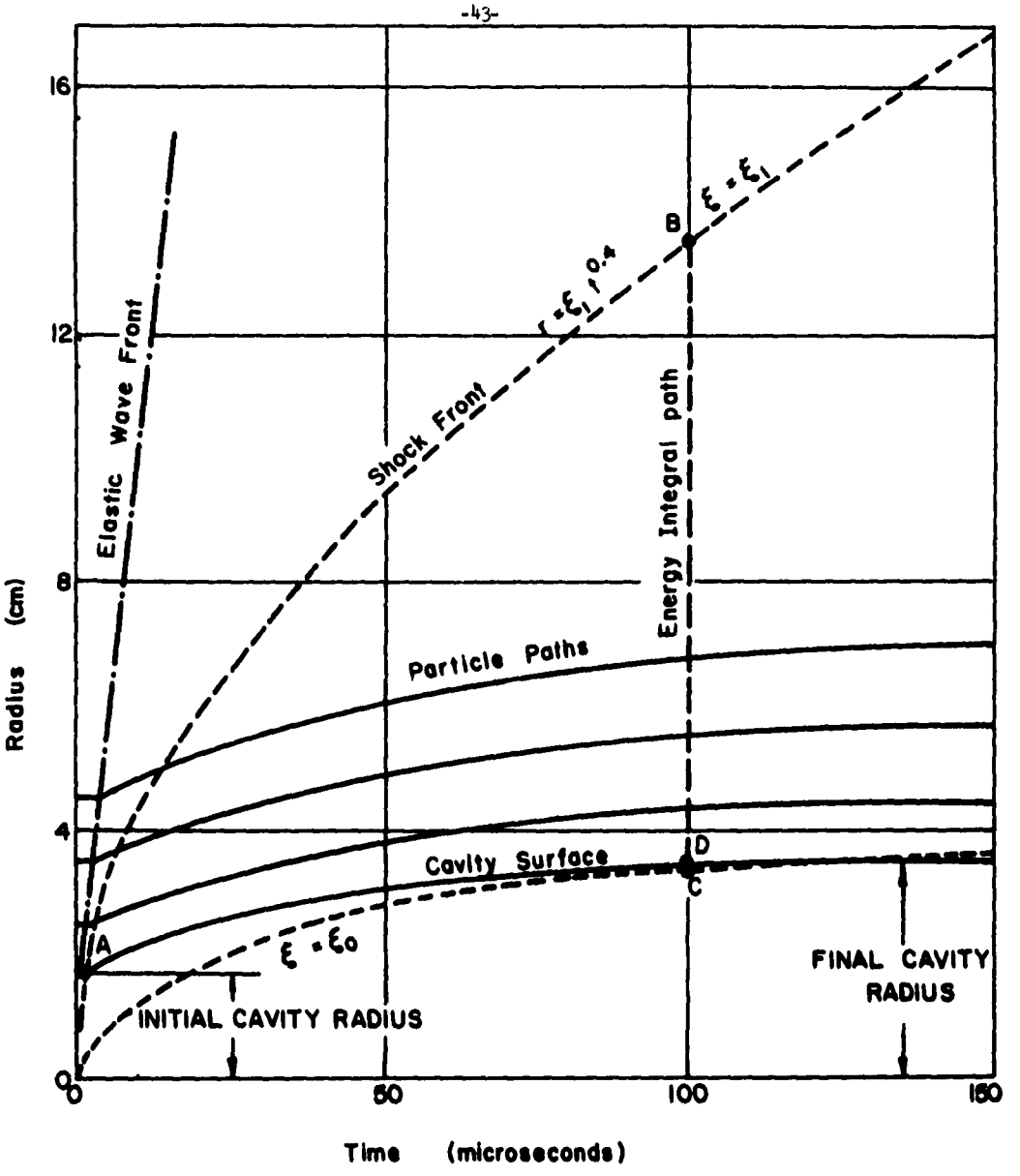

FIG 3 - CAVITY EXPANSION AND PARTICLE TRAJECTORIES

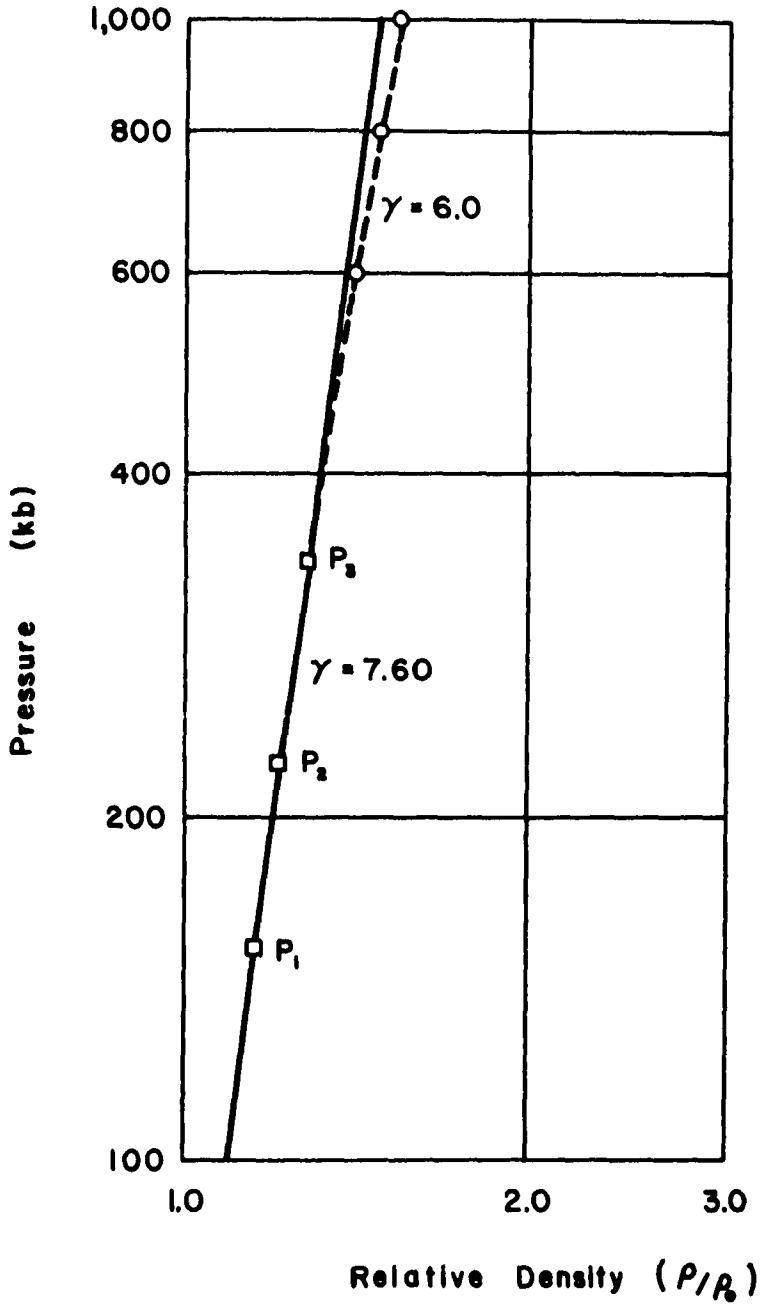

FIG. 4 - EQUATION OF STATE OF ALUMINUM

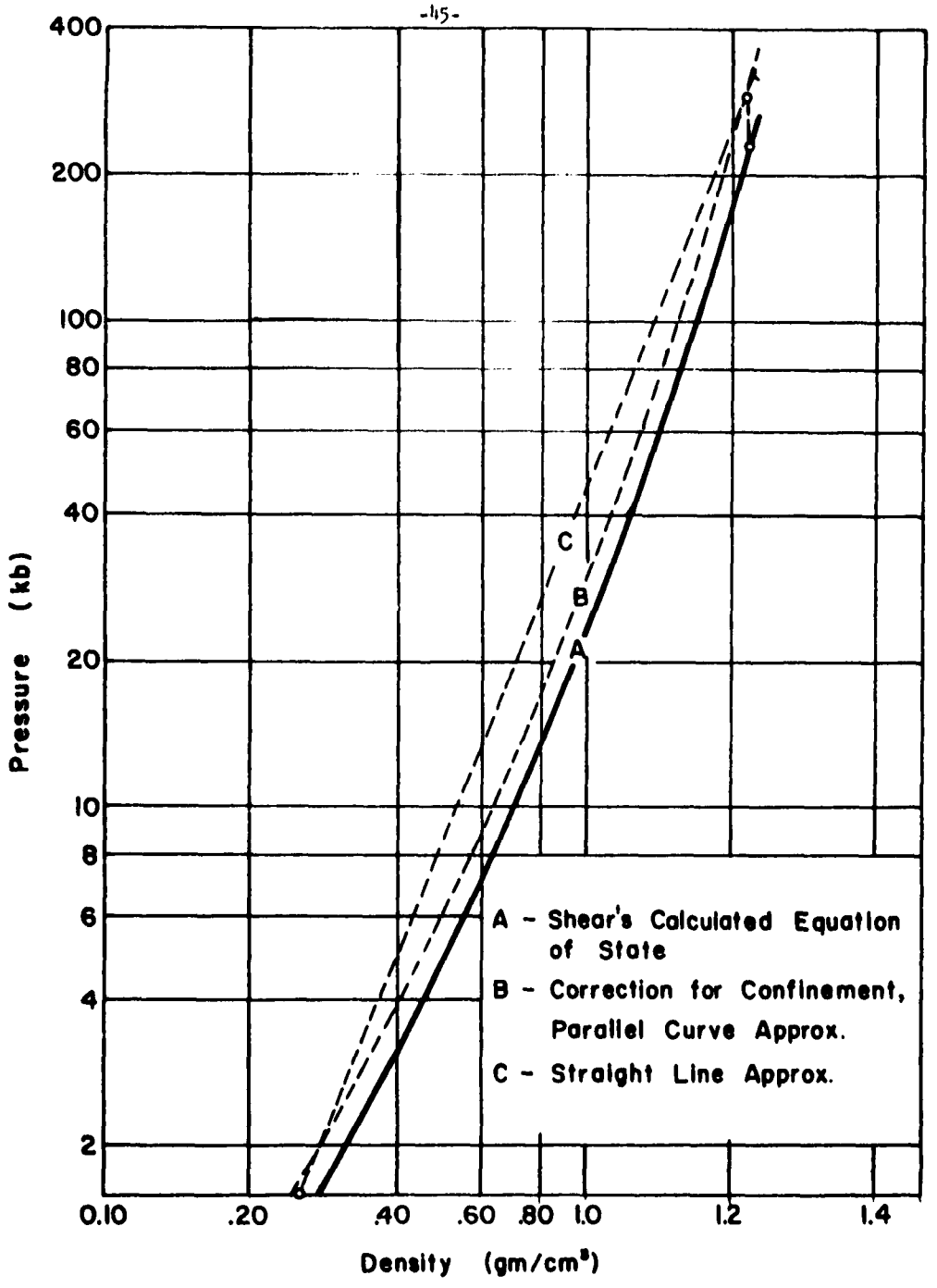

FIG 5 - EQUATION OF STATE, EXPLOSION PRODUCTS OF PENTOLITE (R. E. SHEAR)

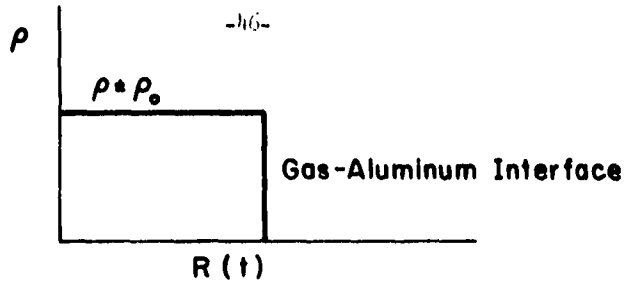

(a) Uniform Density

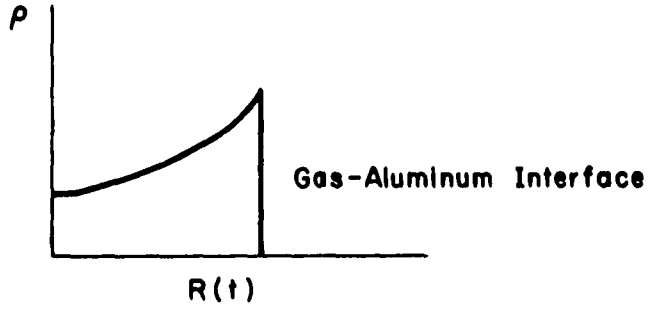

(b) Nonuniform, Detonation Wave Remains in Contact With Metal Boundary

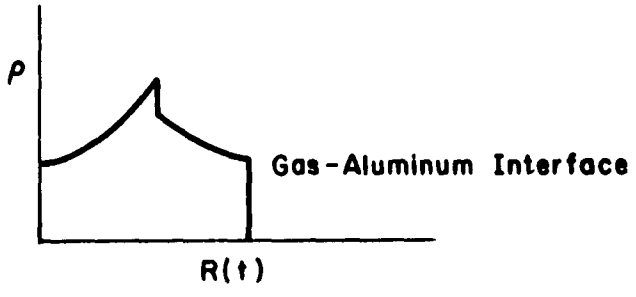

(c) Detonation Wave Reflected from Metal Boundary

FIG. 6 - POSSIBLE MODELS FOR DENSITY VARIATION OF GAS IN EXPANDING CAVITY

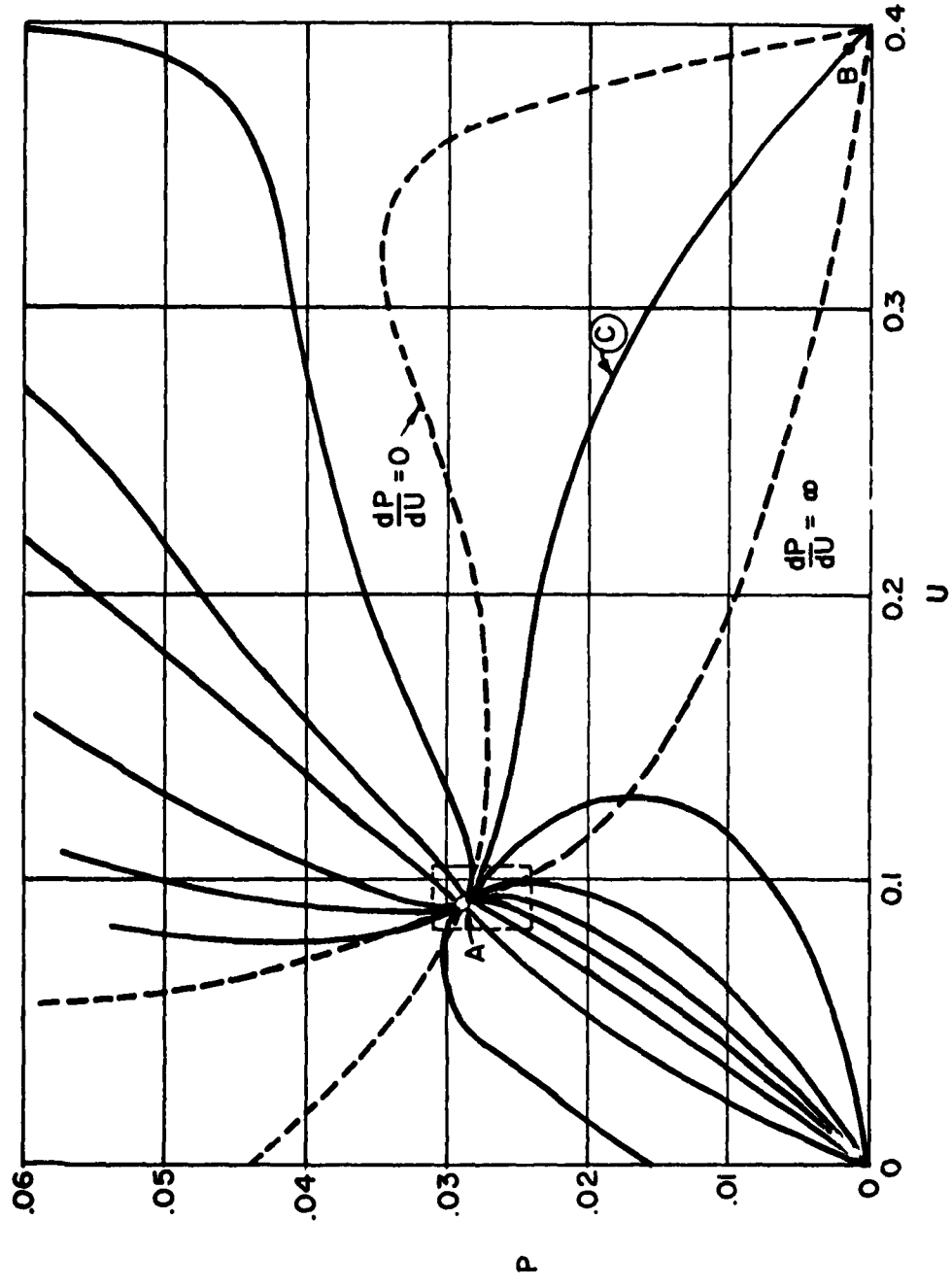

FIG 7 - P,U DIAGRAM, PROGRESSING WAVES : AL, $\gamma = 7.6$

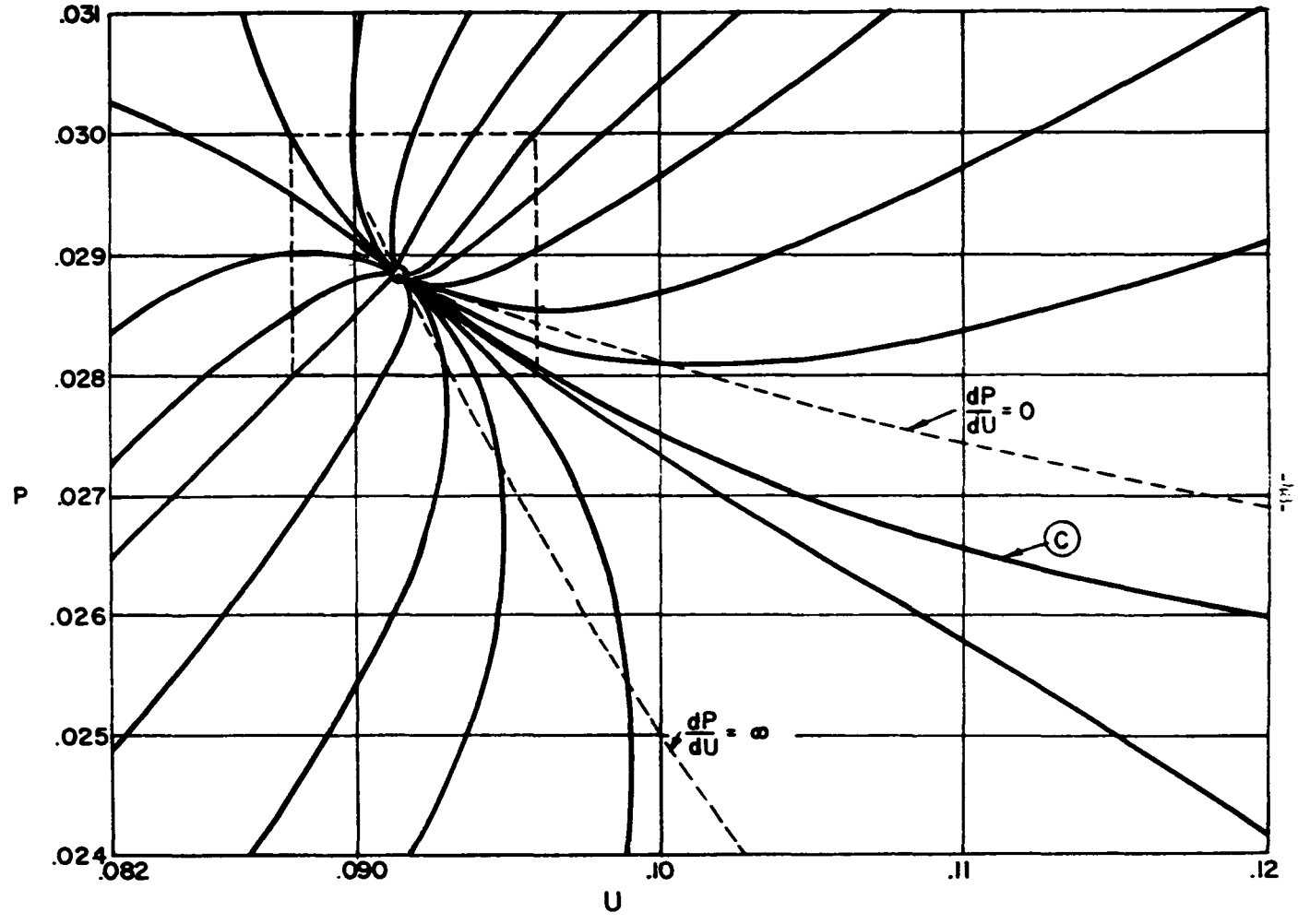

FIG 8 - BEHAVIOR OF SOLUTION CURVES NEAR U=.0916, P=.02884 for $\gamma = 7,6$

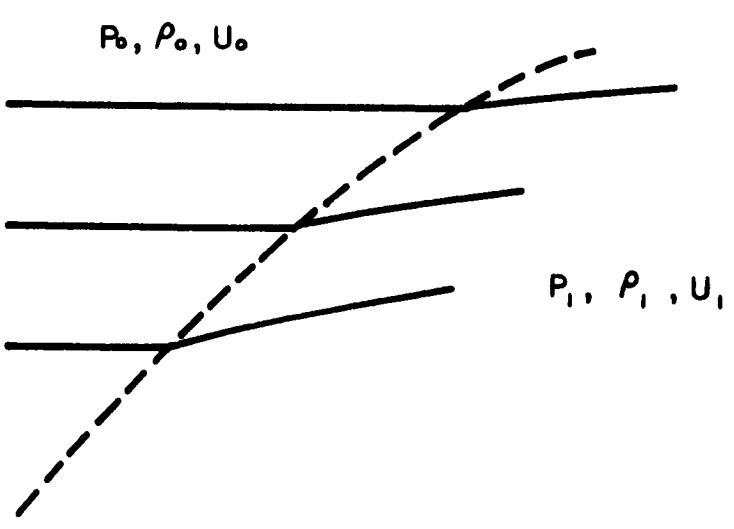

(a) FINITE SHOCK STRENGTH

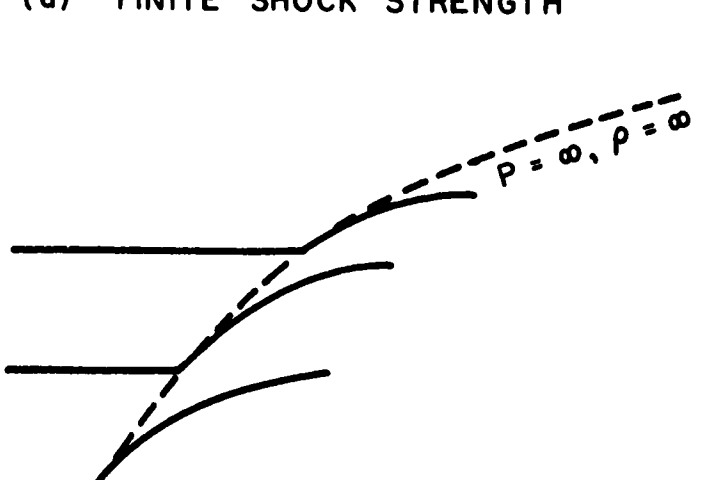

(b) INFINITE SHOCK STRENGTH

FIG. 9 - POSTULATED PARTICLE PATHS ACROSS SHOCK FRONTS.

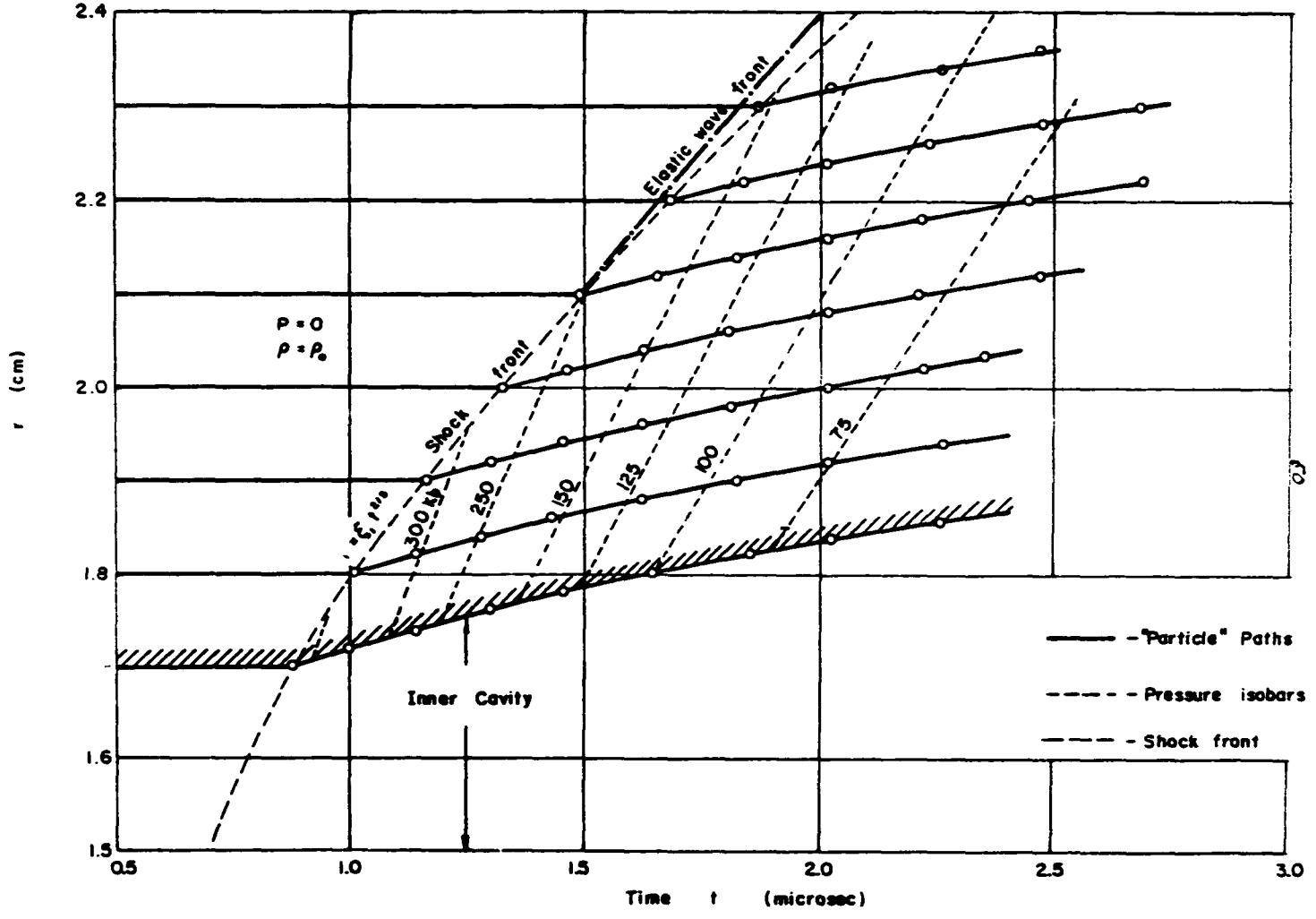

FIG. 10 - r, t - DIAGRAM OF SHOCK REGION FOR ALUMINUM SPHERE

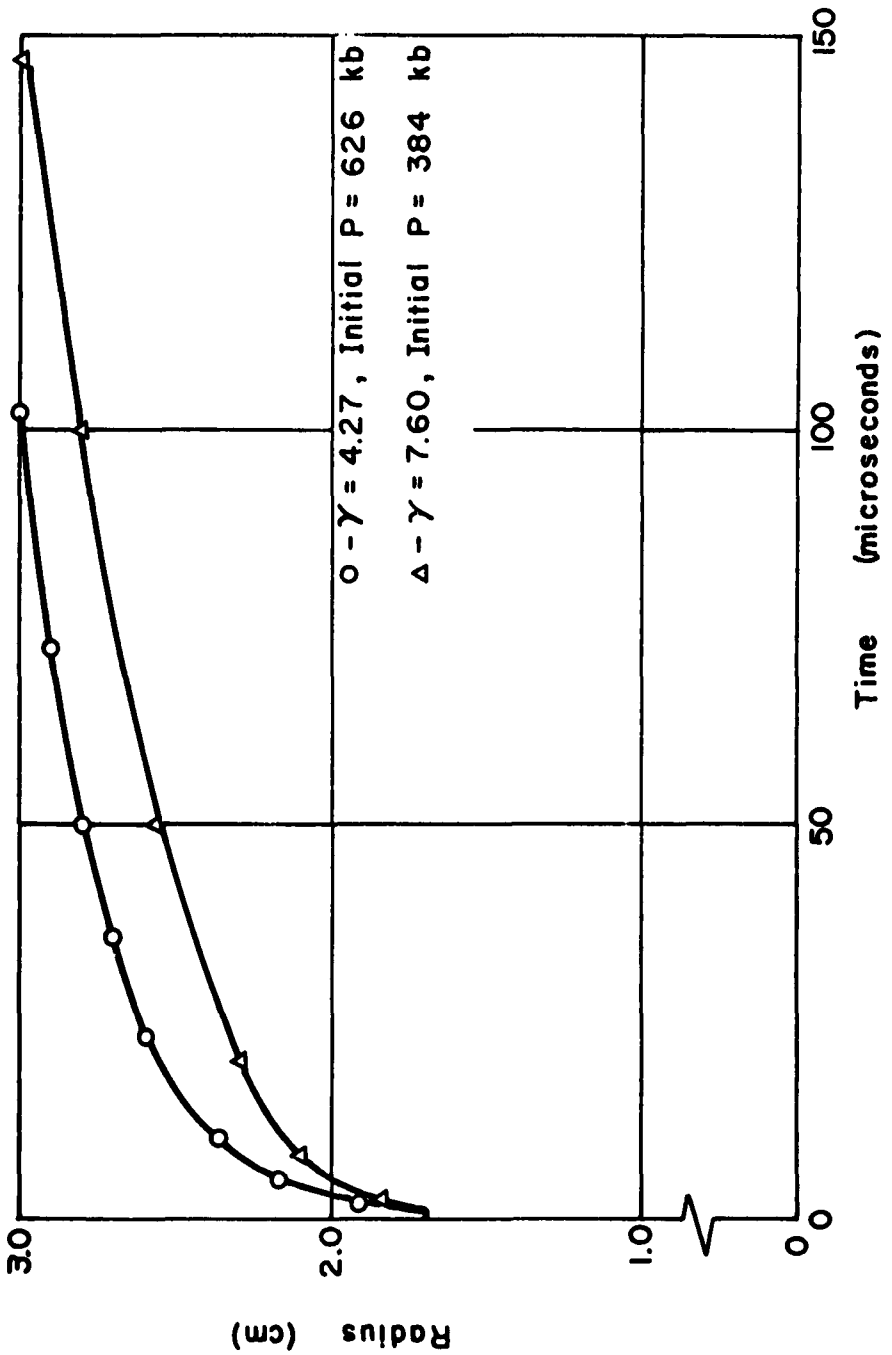

FIG. 11 - R-T DIAGRAM FOR CAVITY SURFACE FOR DIFFERENT γ'S

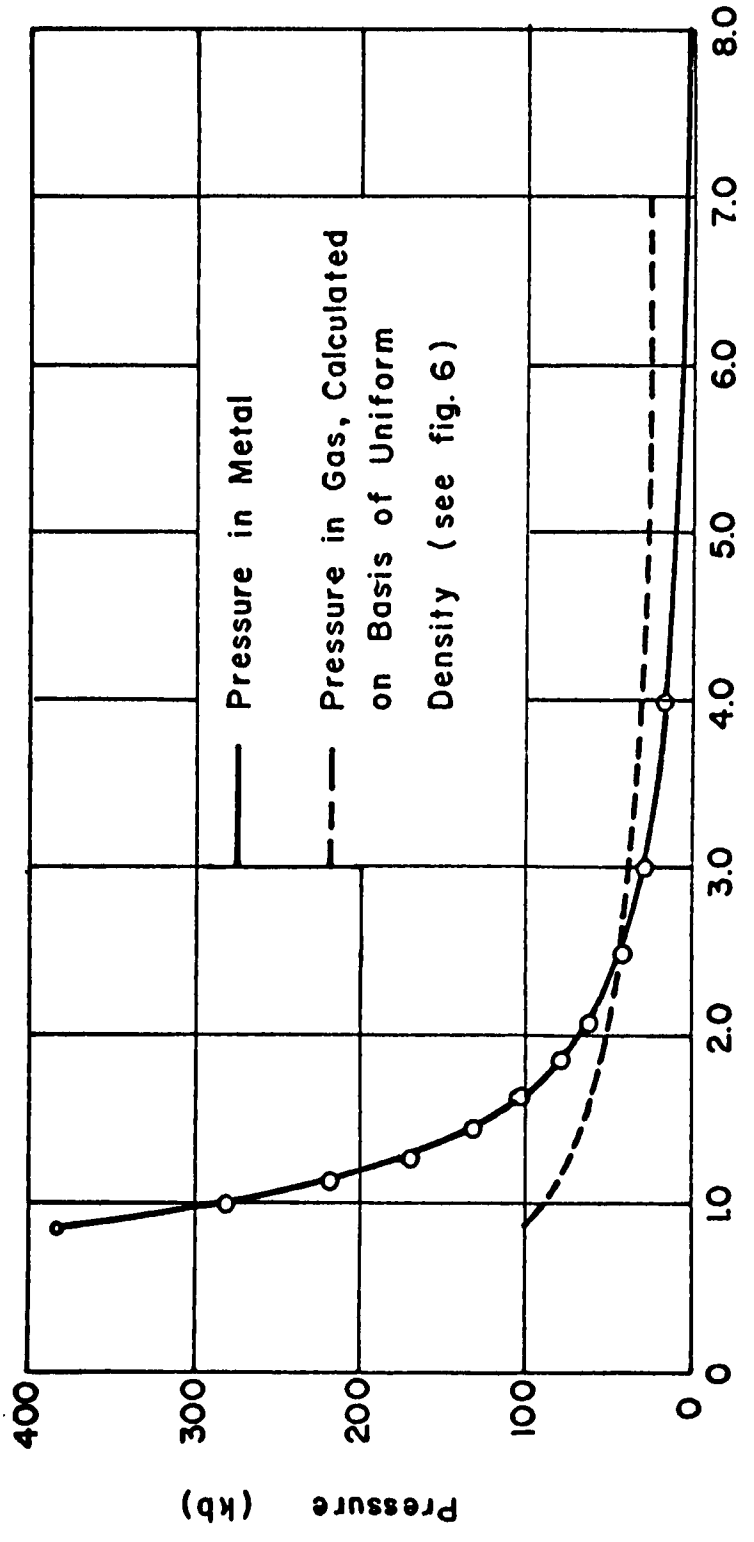

FIG. 12 - PRESSURE DECAY ON CAVITY SURFACE IN AL :
$\gamma = 7.6$, $\rho = 2.70$ gm/cm^3

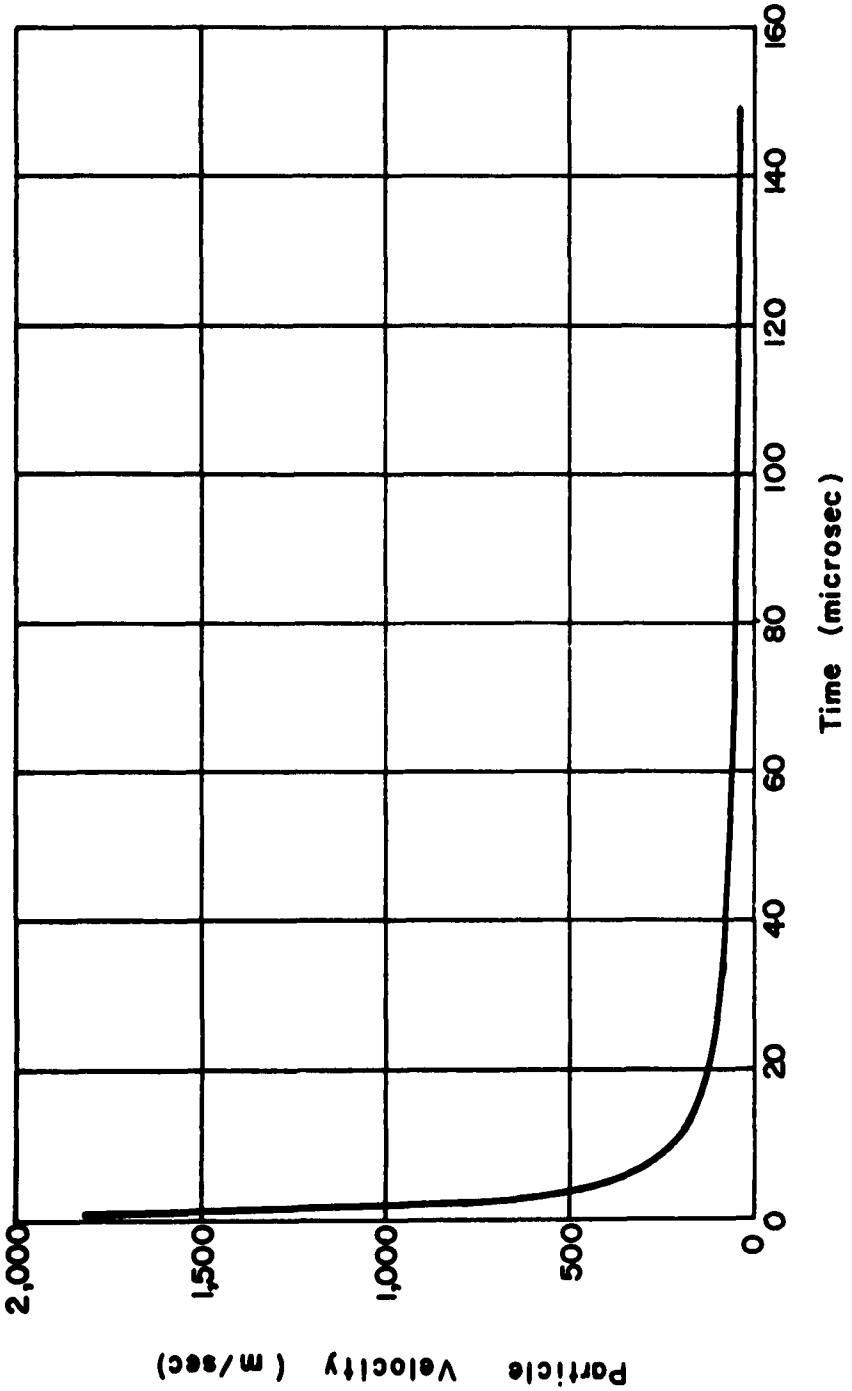

FIG 13 - PARTICLE VELOCITY ON CAVITY SURFACE
AL : $\gamma = 7.6$, $\rho_o = 2.70$ gm/cm^3

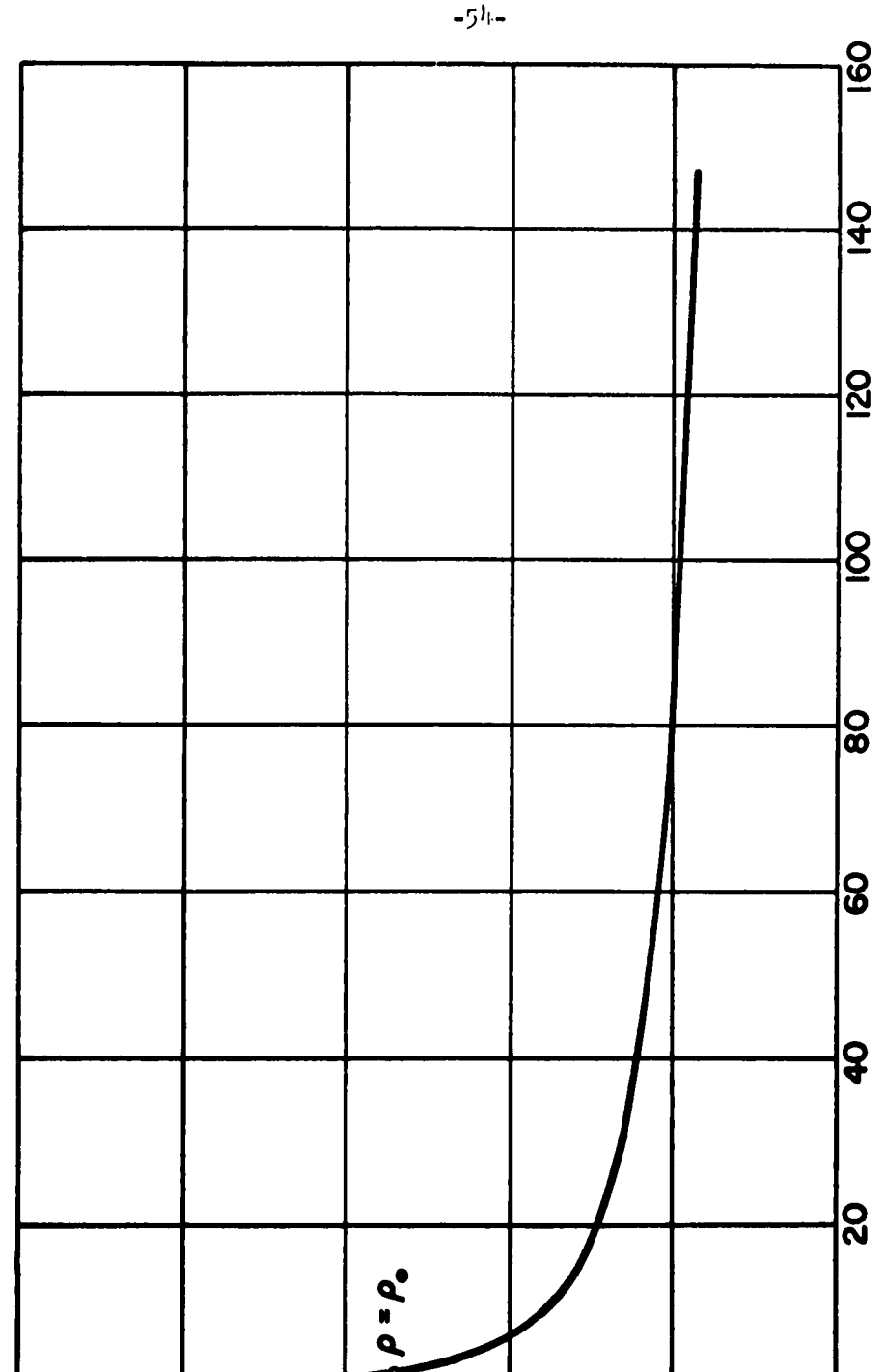

FIG 14 – VARIATION OF DENSITY AT CAVITY SURFACE ;

AL : $\gamma = 7.6$ $\rho_0 = 2.70$ gm/cm^3